New trend of superconductivity in strongly correlated electron systems

2007 J. Phys.: Condens. Matter 19 125201

(http://iopscience.iop.org/0953-8984/19/12/125201)

IOP PUBLISHING JOURNAL OF PHYSICS: CONDENSED MATTER

J. Phys.: Condens. Matter **19** (2007) 125201 (30pp) doi:10.1088/0953-8984/19/12/125201

New trend of superconductivity in strongly correlated electron systems

K Miyake

Division of Materials Physics, Department of Materials Engineering Science, Graduate School of Engineering Science, Osaka University, Toyonaka, Osaka 560-8531, Japan

E-mail: miyake@mp.es.osaka-u.ac.jp

Received 3 January 2007
Published 6 March 2007
Online at stacks.iop.org/JPhysCM/19/125201

Abstract

A new trend in the theory of heavy-fermion superconductivity is reviewed, paying attention to the role of critical valence fluctuations (CVFs). First of all, the trends of superconducting mechanisms of electronic (repulsive) origin are briefly summarized. Secondly, it is discussed that the pressure induced enhancement of the superconducting transition temperature T_c and associated anomalies observed in $CeCu_2(Ge, Si)_2$ can be understood in a unified way by a single assumption that the systems are subject to the critical valence transition of the Ce ion by the pressure tuning. Thirdly, it is shown that the extended periodic Anderson model with the repulsion between f and conduction electrons really has the potentiality of such a sharp valence transition of Ce ions containing f electrons. In particular, enhancement of the residual resistivity, the Sommerfeld constant and T_c, and T-linear resistivity, are shown to be concluded from this model. Fourthly, the locality of this CVF is briefly discussed. Fifthly, it is argued that CVF is enhanced by the magnetic field when the system is located near the critical point of valence transition in relation to the case of $CeCu_6$. Finally, it is argued that the CVF mechanism is a rather universal one which may be related to the physics of Ce115 and Pu115 compounds as well.

(Some figures in this article are in colour only in the electronic version)

1. Introduction—trends of unconventional superconductivity

Since the discovery of the paramagnon mechanism of Cooper pair formation in superfluid ^{3}He in the early 1970s [1, 2], the electronic mechanism of superconductivity has been widely recognized in the 1980s through the discovery of unconventional superconductivity in heavy-fermion compounds $CeCu_2Si_2$, which later turned out to be located near the antiferromagnetic (AF) phase boundary [3]. In particular, it was proposed first in heavy-fermion superconductivity that the AF spin-fluctuation mechanism works in Ce-based heavy

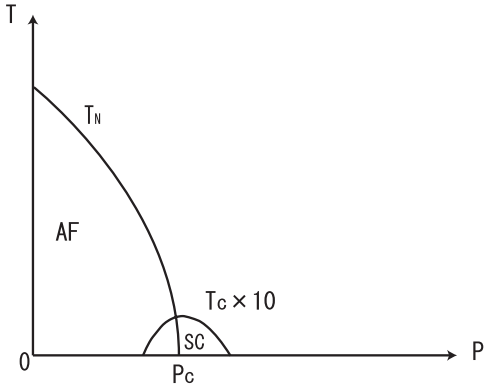

Figure 1. Schematic P–T phase diagram for CeT_2Si_2 (T = Pd, Rh) and $CeIn_3$ showing rather low T_c in a very narrow range of $P \sim P_c$. The T dependence of the resistivity follows the non-Fermi liquid law $\rho(T) \sim T^n$, with $n \simeq 1.5$. It is noted that the scale of T_c is expanded tenfold.

fermions [4, 5], and later on that it also works in high-T_c cuprates [6, 7], and some organic metals which are all in proximity to the AF ordered state [8].

In the 1990s, the pressure induced superconducting phase has been identified near the AF quantum critical point (QCP) in a series of Ce-based heavy-fermion compounds, such as $CeIn_3$ [9], $CePd_2Si_2$ [10], and $CeRh_2Si_2$ [11] as shown in figure 1, where the AF spin-fluctuation mechanism is also considered to work [12]. Let us classify these compounds into class (I).

From the theoretical point of view, these spin-fluctuation mechanisms can be regarded as extensions of the Kohn–Luttinger idea in which the pairing interaction is shown to be induced in an anisotropic channel by the second-order perturbation process on the basis of the Hubbard model [13]. Recently, effects of higher-order perturbation on the pairing interaction have been studied as a model of high-T_c cuprates [14] and Sr_2RuO_4 [15].

On the other hand, the superconducting mechanism of U-based heavy fermions together with Pr-based filled skutterudite [16], which have a plural number of f electrons, seems to have aspects somewhat different from that of Ce-based ones. Even their normal state properties are quite different from Ce-based heavy fermions. For instance, UPt_3 exhibits a very unusual Fermi liquid state [17–19] apart from the multiphase of the superconducting state [20]; UPd_2Al_3, which exhibits the itinerant–localized dual nature of plural f electrons, is proposed to be mediated by 'magnetic excitons' [21, 22]; pressure induced ferromagnetic superconductor UGe_2 [23–25] appears near another phase boundary located deep in the ferromagnetic phase and seems to be related to metamagnetic behaviour triggered by combined SDW–CDW fluctuations there [26]. In any case, the superconducting mechanisms of f^2-based heavy fermions are far from true understanding.

In parallel to these developments, apparently different behaviour of T_c against the pressure P was found in $CeCu_2Si_2$ and $CeCu_2Ge_2$. In particular, for $CeCu_2Si_2$, it was found even at quite an early stage of research [27], while extensive research restarted in the mid-1990s. Both compounds exhibit a pronounced dome of T_c at P far above P_c, which corresponds to the AF-QCP: T_c exhibits a broad peak at around $P \simeq 5$ GPa for $CeCu_2Si_2$ [27, 28], and at around $P \simeq 16$ GPa for $CeCu_2Ge_2$ [29–31]. These isostructural compounds have a similar phase diagram in the P–T plane and similar physical properties, if the origin of the pressure is shifted by about 12 GPa [32]. The schematic behaviour of T_c against the pressure P is illustrated in

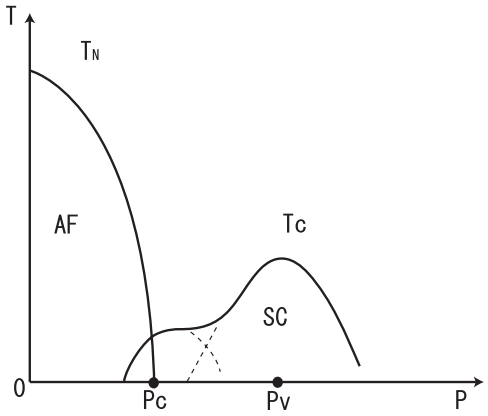

Figure 2. Schematic P–T phase diagram for $CeCu_2(Si/Ge)_2$ showing the two critical pressures P_c and P_v. At P_c, where the Néel temperature $T_N \to 0$, superconductivity in region SC I is mediated by AF spin fluctuations; around P_v, in the region SC II, critical valence fluctuations provide the pairing mechanism. At $T > T_{SC\,II}$, the resistivity is linear in temperature.

figure 2. Around the pressure where T_c takes a maximum, they exhibit a drastic decrease of the coefficient A of the T^2 term of the resistivity, $\rho(T) = \rho_0 + AT^2$ and sharp enhancement of the residual resistivity ρ_0. Let us classify these compounds into a class (II).

From research activities over several years, it turned out that these phenomena, observed in materials of class (II), have a single origin of the critical valence transition (CVT) of the Ce ion at $P = P_v$ [33–35], while it was suggested that the enhancement of T_c is related to the valence transition of the Ce ion from the first stage of research [27]. The T-linear resistivity is observed in a wide temperature region up to a few 10 K except for the very low temperature region, which clearly shows that the universality class of the QCP at $P = P_v$ is different from that of the AF-QCP [30, 31]. It is also noted that T_c of the canonical class (I), shown in figure 1, is far lower than the present case (shown in figure 2).

This novel point of view was reinforced by two recent experiments. First, the two separate domes of T_c was observed in $CeCu_2(Si_{0.9}Ge_{0.1})_2$, one at around $P \sim P_c$ and one $P \sim P_v$ [36], suggest the existence of two different mechanisms related to fluctuations associated with two different QCPs, one for the AF-QCP and another for the QCP associated with the CVT. It was also revealed that T_c around P_c is lower than that around P_v by about half. Second, the detailed and fine experiments of $CeCu_2Si_2$ under pressure were performed including measurements of the specific heat in addition to the resistivity [37], and their results were successfully explained by the theory which allows the CVT and fluctuations [34, 35]. Thus, the critical-valence–fluctuation mechanism, a new mechanism of superconductivity of electronic origin, was identified both experimentally and theoretically.

The so-called Ce115 compounds, $CeTIn_5$ (T = Rh [38], Co [39], Ir [40]) [41], seem to have both aspects of class (I) and (II). Namely, P_c and P_v do not seem to be well separated.

Another new development of unconventional superconductivity is that the intrinsically gapless superconductivity was found in $CeCu_2Si_2$ [42] and $CeRhIn_5$ [43] under a rather narrow pressure range around the AF-QCP where the AF order and superconductivity coexist microscopically. This novel state of superconductivity was explained as a realization of the so-called odd-frequency gap state [44] which was shown to be possible [45] in the paramagnetic state very close to the AF-QCP and the AF ordered state near the AF-QCP on the basis of the itinerant–localized duality model of the Ce-based heavy fermions [46]. Indeed, it was shown

by an explicit calculation of T_c that the 'p-wave singlet' odd-gap state dominates over the *conventional* d-wave singlet state in such a region around the AF-QCP [45].

The purpose of this paper is to summarize our previous results to give a comprehensive viewpoint of the critical-valence–fluctuation mechanism of unconventional superconductivity, and to add recent consideration on the origin of the critical-valence–fluctuation phenomena from a more physical point of view. In section 2, we give a qualitative description of the CVT and its consequences, paying attention to the case of $CeCu_2Ge_2$, in which all the ingredients of these phenomena appear. In section 3, we summarize the results by the microscopic theory, which predicts the existence of the CVT, and peaks of the superconducting transition temperature T_c and the residual resistivity ρ_0, the enhancement of the Sommerfeld constant $\gamma(T) \equiv C(T)/T$ at around the CVT point. It is also discussed why the T-linear resistivity is observed at the CVT point, and that its origin is the locality of CVT phenomena, which also explains why the d-wave pairing is induced by critical valence fluctuations (CVFs). In section 4, we discuss the reason why the locality of CVF follows in the strongly correlated Ce-based heavy fermions. In section 5, we argue that this CVF mechanism is rather universal and can be the origin of unconventional superconductivity of other compounds under pressure, such as that of Ce115 compounds. Finally, in section 6, we discuss the effect of the magnetic field on the CVT and the possibility of emergence of the CVT in $CeCu_6$ due to the magnetic field of attainable strength to date.

2. Qualitative description of phenomena associated with the critical valence transition

2.1. Quantum critical valence transition

The qualitative difference in the P-dependence of T_c in figures 1 and 2 suggests that the superconducting mechanism at around $P \sim P_v$ is different from that at around $P \sim P_c$. In particular, the pressure corresponding to the large peak of T_c is located on the higher pressure side far away from P_c corresponding to the AF-QCP, which denies the AF spin-fluctuation mechanism for the appearance of the T_c peak if one consults the strong-coupling theory based on a phenomenological spin-fluctuation spectrum [12]. This point of view is supported further by the following experimental results in $CeCu_2Ge_2$ [29].

Firstly, the A coefficient of the T^2 resistivity law decreases drastically by about two orders of magnitude around the pressure $P = P_v$ corresponding to the T_c peak. Since A scales as $(m^*/m)^2$ in the so-called Kondo regime, this implies that the effective mass m^* of the quasiparticles also decreases sharply there. This fall of m^* is possible only if there is a sharp change of valence of Ce, deviating from Ce^{3+}, since the following approximate formula holds in the strongly correlated limit [47, 48]:

$$\frac{m^*}{m} = \frac{1 - n_f/2}{1 - n_f}, \tag{1}$$

where n_f is the f-electron number per Ce ion. It is also noted that the resistivity follows T-linear dependence in the wide temperature regime $T > T_{SC\,II}$, in contrast to the case of compounds of class (I) where $\rho(T) \sim T^n$ with $n \simeq 1.5$. This turned out to be a signature of quantum CVT [37].

Second, the so-called Kadowaki–Woods (KW) ratio [49], A/γ^2, where γ is the Sommerfeld coefficient of the electronic specific heat, crosses over quickly from that of a strongly correlated class to a weakly correlated one. γ^{-1} can be identified with the Kondo temperature T_K, which is experimentally accessible by resistivity measurements. This indicates that the mass enhancement due to the dynamical electron correlation is quickly lost at around

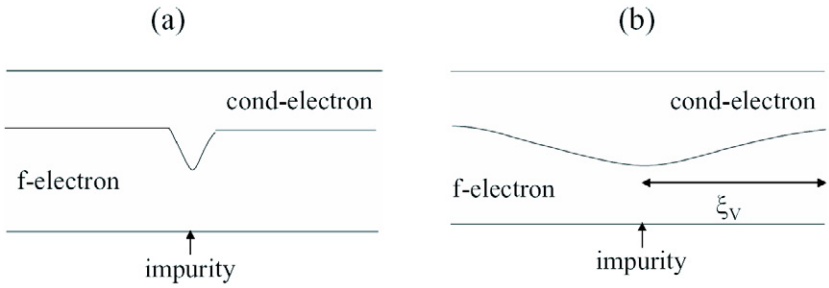

Figure 3. Schematic view of the charge distribution of f and conduction electrons around an impurity: (a) far from $P \sim P_v$, where the effect of the impurity remains short ranged so that the residual resistivity ρ_0 is not enhanced; (b) at around $P \sim P_v$, where the effect of the impurity extends to the long-range region, because the correlation length ξ_v of valence fluctuations diverges as $P \to P_v$, leading to highly enhanced ρ_0.

$P \sim P_v$ [50], in agreement with the previous point. The phenomenon can be understood if we note the fact that γ consists essentially of two terms:

$$\gamma = \gamma_{band}\left(1 - \frac{\partial \Sigma(\epsilon)}{\partial \epsilon}\right) \equiv \gamma_{band} + \gamma_{cor}, \tag{2}$$

where γ_{band} is due to the so-called band effect and $\gamma_{cor} \equiv -\gamma_{band}\partial\Sigma(\epsilon)/\partial\epsilon$ is due to the many-body correlation effect, with $\Sigma(\epsilon)$ being self-energy of correlated electrons. γ_{cor} and the A coefficient are related to each other through the Kramers–Krönig relation, leading to the large value of the KW ratio [50]. If $\gamma_{cor} \gg \gamma_{band}$, the KW ratio is attained. On the other hand, if $\gamma_{cor} \sim \gamma_{band}$, the ratio A/γ^2 should be reduced from the KW value considerably because the effect of the γ_{band} cannot be neglected in its denominator [51].

Third, the sharp peak of the residual resistivity ρ_0 at around $P \sim P_v$ can be understood as a many-body effect enhancing the impurity potential. In the forward scattering limit, this enhancement is proportional to the valence susceptibility $-(\partial n_f/\partial \epsilon_f)_\mu$, where ϵ_f is the atomic f-level of the Ce ion, and μ is the chemical potential [35]. Physically speaking, local valence change coupled to the impurity or disorder gives rise to the change of valence in a wide region around the impurity which then scatters the quasiparticles quite strongly, leading to the increase of ρ_0 (see figure 3). It is noted that the effect of AF critical fluctuations on ρ_0 is rather moderate [52]. The enhancement of ρ_0 can thus be directly related to the degree of sharpness of the valence change because the variation of the atomic level ϵ_f is considered to be a smooth function of the pressure. The critical pressure P_v is indeed defined by the maximum of ρ_0.

Finally, the rapid volume change maintaining the crystal symmetry was reported near $P \sim P_v$ by x-ray diffraction using a source of synchrotron orbit radiation, implying that the rapid valence change occurs there [53].

A similar trend has recently been observed in $CeCu_2Si_2$ [37]. The summary of the results of [37] is reproduced in figure 4. The aspects observed in $CeCu_2Ge_2$ are essentially the same except for the origin of the pressure gauge (see figure 2).

Thus, it seems reasonable to seek the origin of the peak of T_c in the rapid change of valence of the Ce ion from the trivalent state to the tetravalent side [33]. The drastic change of valence has been known as the valence transition for almost half a century. A typical example is the α–γ transition in Ce metal [54], which is a first-order transition with a critical point (T_{cr}, P_{cr}) as in the case of the conventional liquid–gas transition. Valence transition phenomena have long been a subject of a community of strongly correlated electron systems based on f-electron compounds [55]. A trend of schematic phase diagrams in the P–T plane is shown in figure 5.

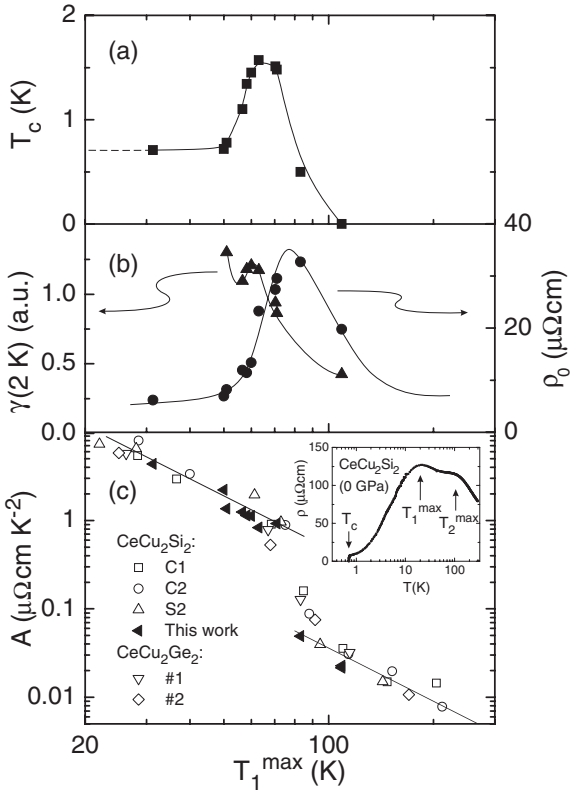

Figure 4. Plotted against $T_1^{\max}$ (defined in the inset), a measure of the characteristic energy scale of the system, are (a) the bulk superconducting transition temperature, (b) the residual resistivity and γ coefficient of the electronic specific heat, and (c) the coefficient A of the $\rho \sim AT^2$ law of resistivity. Note the straight lines where the expected $A \propto (T_1^{\max})^{-2}$ scaling is followed. The maximum of T_c coincides with the start of the region where the scaling relation is broken, while the maximum in residual resistivity is situated in the middle of the collapse in A. Pressure increases towards the right-hand side of the scale (high T_K) [37].

In the typical case, the critical point is located at finite temperature T_{cr}, which is far larger than the effective Fermi energy ϵ_F^* in heavy fermions. However, there is a possibility that $T_{cr} = 0$ at some pressure P_v where the quantum CVT occurs and the CVFs develop around there. Enhanced valence fluctuations are expected to develop even though $T_{cr} > 0$ as far as $T_{cr} \ll \epsilon_F^*$.

2.2. Model allowing quantum critical valence transition

The periodic Anderson model (PAM), which is considered to be a good model for heavy-fermion metals, does not exhibit such a CVT no matter how the parameters are chosen. The effect of pressure is twofold; one is to increase the hybridization V between f and conduction electrons, and another is to shift the f level ϵ_f relative to the Fermi level ϵ_F, so as to approach ϵ_F in Ce-based compounds. Indeed, these variations of parameters themselves cannot cause the drastic change of valence of the Ce ion from that of the Kondo regime to the VF regime, although the valence increases prominently as V is increased or the level ϵ_f is increased, approaching the Fermi level [56]. In order for such a sharp valence transition to occur, we need

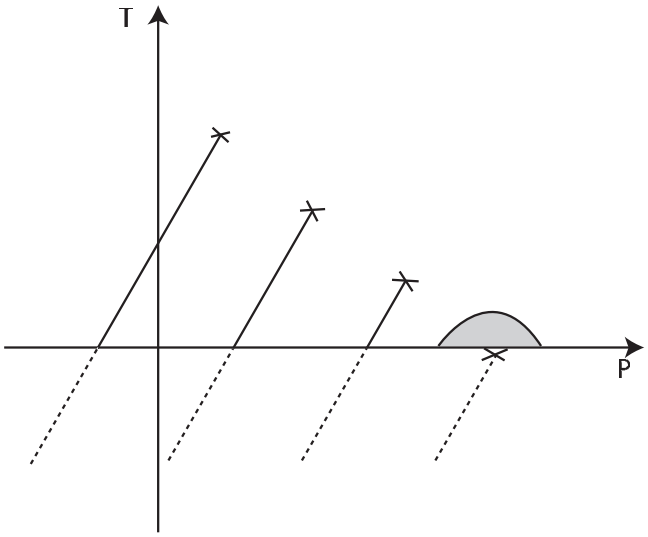

Figure 5. Schematic P–T phase diagram of typical valence transition in Ce-based compounds, where $T_{\rm v}(P)$ denotes the phase boundary and crosses denote the critical end point ($T_{\rm cr}$, $P_{\rm cr}$). There are two cases, $T_{\rm v}(P=0) > 0$ or $T_{\rm v}(P=0) < 0$. As a special case of the latter, a case where $T_{\rm cr} = 0$ or $T_{\rm cr} \lesssim 0$ is possible. In such a case, CVFs develop in the low temperature region at $P \sim P_{\rm v}$, where $T_{\rm cr}(P_{\rm v}) = 0$, as indicated by the shaded region.

to take into account the repulsion $U_{\rm fc}$ between f and conduction electrons [55, 57]. Namely, the PAM should be extended as follows:

$$\mathcal{H} = \sum_{k\sigma}(\epsilon_k - \mu)c^\dagger_{k\sigma}c_{k\sigma} + \epsilon_{\rm f}\sum_{k\sigma} f^\dagger_{k\sigma}f_{k\sigma} + U_{\rm ff}\sum_i n^{\rm f}_{i\uparrow}n^{\rm f}_{i\downarrow} + V\sum_{k\sigma}(c^\dagger_{k\sigma}f_{k\sigma} + {\rm h.c.}) + U_{\rm fc}\sum_{i\sigma\sigma'} n^{\rm f}_{i\sigma}n^{\rm c}_{i\sigma'}, \tag{3}$$

where the conventional notations for the PAM are used except for $U_{\rm fc}$, the f–c Coulomb repulsion.

The effect of $U_{\rm fc}$ on the valence change of the Ce ion has been discussed in a number of contexts and models. With regard to the impurity Anderson model, the effect of $U_{\rm fc}$ was discussed in relation to optical experiments, valence-band photoemission (PES) and bremsstrahlung isochromat spectroscopy (BIS) [58–61]. Costi and Hewson studied the effects of $U_{\rm fc}$ by a numerical renormalization group (NRG) approach [60, 61]. They concluded that in the Kondo regimes $U_{\rm fc}$ can be absorbed into other parameters (V, $\epsilon_{\rm f}$ and $U_{\rm ff}$), and the same set of renormalized parameters on $U_{\rm fc} = 0$ is consistent with both the valence-band PES and BIS spectra and the thermodynamic properties. The effect of increasing $U_{\rm fc}$ is to increase the Kondo temperature, thus to decrease the number of f electrons $n_{\rm f}$ per ion more rapidly. Indeed, a related model has been investigated on the basis of the NRG approach by Takayama and Sakai, and it turned out that $n_{\rm f}$ rapidly decreases at $\epsilon_{\rm f} \approx E_{\rm F} - U_{\rm fc}$, $E_{\rm F}$ being the Fermi level, as $\epsilon_{\rm f}$ is increased so as to approach $E_{\rm F}$ [62]. This result implies that the rapid valence change occurs where $\epsilon_{\rm f} + U_{\rm fc}$, the energy of the f^1 state, and $E_{\rm F}$, the energy of the state f^0+ (extra conduction electron on the Fermi level), are nearly degenerate, giving rise to enhanced valence fluctuations. Then, $U_{\rm fc}$ has a considerable effect on the valence fluctuation, although it does not cause a critical valence instability in the impurity Anderson model.

It is not easy to examine the effects of U_{fc} in the PAM due to the lattice effect in general. In the case of the impurity model, the conduction band plays the role of an electron bath so that the chemical potential μ is essentially fixed. However, in the case of the lattice model, μ is considerably affected by U_{fc} itself so that we have to treat the problem in a self-consistent fashion. In particular, such a self-consistent treatment is indispensable when the valence state of Ce begins to leave the Kondo regime to the VF one under high pressure. In the physical picture, however, the condition for the valence transition may be still given by that of the degeneracy of two valence states of Ce, $Ce^{3+} \rightleftharpoons Ce^{4+}$:

$$\epsilon_f + U_{fc}\langle n_c \rangle \approx E_F, \tag{4}$$

where $\langle n_c \rangle$ is the average number of conduction electrons at each f site. There exist some studies of the extended PAM with U_{fc} within Hartree–Fock-like approximations [63–65]. Even in this simple level of approximation, U_{fc} is responsible for the rapid change of the number of f electrons as the level ϵ_f is tuned, leading to the first order transition in the large U_{fc} region. Then, by tuning the strength of U_{fc}, it is possible to reduce the critical end point associated with valence transition down to zero temperature, where quantum critical fluctuations should prevail.

We studied the extended PAM with U_{fc} in one dimension by the variational Monte Carlo method on the extended Gutzwiller variational wavefunction [66], and showed that the valence of f electrons decreases rapidly as the level of f electrons ϵ_f is increased, if U_{fc} is moderately large, comparable to half of the bandwidth of conduction electrons. Quite recently, the same model in one dimension was treated by the density matrix renormalization (DMRG) method, giving asymptotically exact properties beyond the mean-field-like approximations although the physical picture was not greatly altered [67].

The similar effects of the d–p Coulomb interaction in the so-called d–p model have been investigated as a possible charge fluctuation mechanism of the high T_c superconductor [68, 69]. On the other hand, the physics discussed in the present paper is rather different from the 'valence fluctuation mechanism' proposed for heavy electron superconductors in [70].

3. Results on microscopic treatments of extended PAM

3.1. Superconductivity induced by critical valence fluctuations

In [34], the model Hamiltonian (3) with a spherical conduction band was treated by the mean-field approximation in the slave boson formalism to discuss the possibility of valence transition and by the Gaussian fluctuation theory around the mean-field solution to discuss a possible superconducting state. As shown in figure 6, central results of [34] are summarized as follows.

(i) Sharp valence change is caused by the effect of U_{fc} with moderate strength of the order of the bandwidth of conduction electrons, when the f level ϵ_f is tuned to mimic the effect of pressure.
(ii) The superconducting state is induced by the process of exchanging the slave-boson fluctuations for the values of ϵ_f around which the sharp valence change occurs.
(iii) The symmetry of the so-induced superconducting state is d wave if the spherical model is adopted for conduction electrons. However, as seen in the argument below, it is the anisotropic pairing that is induced by the CVF modes due to their *almost local* nature.

It is remarked that aspects of the pressure dependence of T_c and A observed experimentally [30], shown in figure 4 [37], are well reproduced, since ϵ_f simulates the pressure variation. The derivation of these results will be briefly shown hereafter.

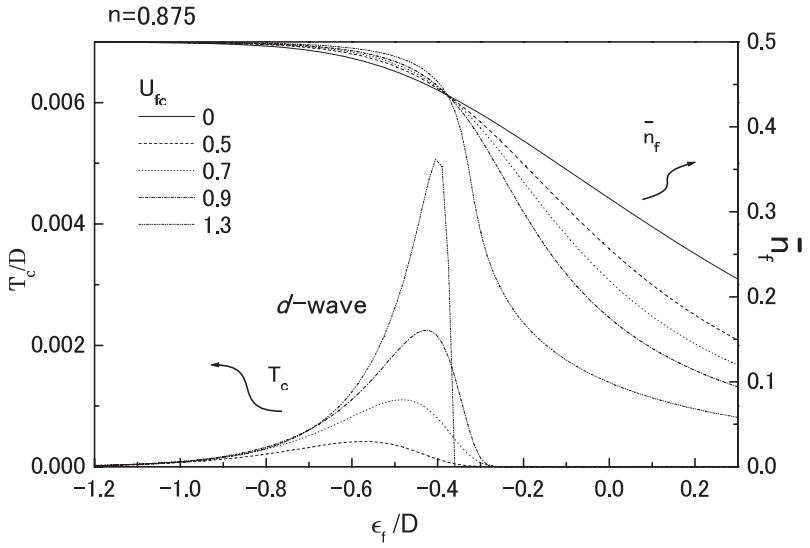

Figure 6. T_c for d-wave channel and $\bar{n}_f$, f-electron number per site and 'spin', as a function of ϵ_f. The total number of electrons per site and 'spin' is set as $n = 0.875$, and the c–f hybridization is set as $V = 0.5D$. The unit of energy is given by D, the Fermi energy of the parabolic conduction band if it were decoupled from f electrons: the dispersion $\epsilon_{\vec{k}} = k^2/2m - D$ is adopted for the conduction electrons.

3.1.1. Mean-field solution for valence change [34]. The Hamiltonian (3) was treated by the *slave-boson* and large-N expansion approach [71–73], which has been shown to be effective for studying thermodynamic properties, superconducting transition temperature, transport properties, etc of the usual PAM [71–77] as far as the low temperature region $T \ll T_K$ is concerned. Following these methods, the effect of the f–c Coulomb interaction in (3) was taken into account on the level of a Gaussian fluctuation approximation.

By generalizing the Hamiltonian (3) to that with the N-hold spin–orbit degeneracy, and assuming the strongly correlation limit, i.e. $U_{ff} \to \infty$, the Hamiltonian is transformed as follows:

$$\mathcal{H} = \sum_{\vec{k}m} \left(\epsilon_k c^\dagger_{\vec{k}m} c_{\vec{k}m} + \epsilon_f f^\dagger_{\vec{k}m} f_{\vec{k}m} \right) + \frac{V}{\sqrt{N_L}} \sum_{\vec{k}\vec{q}m} \left(c^\dagger_{\vec{k}m} f_{\vec{k}+\vec{q}\,m} b^\dagger_{\vec{q}} + \text{h.c.} \right) + U_{fc} \sum_{ilm} f^\dagger_{il} f_{il} c^\dagger_{im} c_{im}, \tag{5}$$

where bs are slave-boson operators describing the f^0 state and the constraint

$$Q_i = \sum_m f^\dagger_{im} f_{im} + b^\dagger_i b_i = 1 \tag{6}$$

is required at each site in order to maintain an equivalence of the truncated Hilbert space and the original one. To generate a $1/N$ expansion variables are written as follows:

$$\begin{aligned} &Q_i \to q_0 N \\ &b \to b\sqrt{N} \\ &V \to V/\sqrt{N} \\ &U_{fc} \to U_{fc}/\sqrt{N}. \end{aligned} \tag{7}$$

In the calculation, the radial gauge was adopted following [71]. (Although the radial and the Cartesian gauge formulations are ultimately equivalent, spurious infrared divergences do not

appear in the radial gauge approach [73].) A local gauge transformation, $b_i(\tau) = \rho_i(\tau)\mathrm{e}^{\mathrm{i}\theta_i(\tau)}$, $f_{im}(\tau) = f'_{im}(\tau)\mathrm{e}^{\mathrm{i}\theta_i(\tau)}$ and $\lambda'_i(\tau) \equiv \lambda_i + \dot{\theta}_i(\tau)$, was performed. Then, the partition function is given as

$$Z = \int \mathcal{D}(cc^\dagger ff^\dagger \rho\lambda)\exp(-S), \tag{8}$$

where the action S is given as

$$\begin{aligned} S = \int_0^\beta \mathrm{d}\tau \Bigg[& \sum_{\vec{k}\vec{k}'m} f^\dagger_{\vec{k}m}(\tau)\{(\partial_\tau + \epsilon_\mathrm{f})\delta_{\vec{k}\vec{k}'} + \frac{1}{\sqrt{N_\mathrm{L}}}\mathrm{i}\lambda(\vec{k}-\vec{k}';\tau)\} f_{\vec{k}'m}(\tau) \\ & + \sum_{\vec{k}m} c^\dagger_{\vec{k}m}(\tau)(\partial_\tau + \epsilon_{\vec{k}})c_{\vec{k}m}(\tau) + \frac{V}{\sqrt{N_\mathrm{L}}}\sum_{\vec{k}\vec{k}'m}\{c_{\vec{k}m}(\tau) f_{\vec{k}'m}(\tau)\rho(\vec{k}-\vec{k}';\tau) + \mathrm{h.c.}\} \\ & + \mathrm{i}\frac{N}{\sqrt{N_\mathrm{L}}}\sum_{\vec{k}\vec{k}'}\rho(-\vec{k}';\tau)\lambda(\vec{k}'-\vec{k};\tau)\rho(\vec{k};\tau) - \mathrm{i}q_0 N\sqrt{N_\mathrm{L}}\lambda(\mathbf{0};\tau) \\ & + \frac{U_\mathrm{fc}}{N}\sum_{ilm} n^\mathrm{f}_{il} n^\mathrm{c}_{im} \Bigg]. \end{aligned} \tag{9}$$

In the above expressions, variables f' and λ' have been rewritten as f and λ, respectively, and the Jacobian factor $\prod_{i\tau}\rho_i(\tau)$ has been neglected following [71].

By introducing two kinds of Stratonovich–Hubbard fields φ^f and φ^c for U_fc, the functional integral over the fermion fields can be performed in equations(8) and (9). Then, the partition function equation (8) can be transformed as follows:

$$Z = \int \mathcal{D}(\rho\lambda\varphi^\mathrm{f}\varphi^\mathrm{c})\exp(-S), \tag{10}$$

$$\begin{aligned} S = & -N\,\mathrm{Tr}(\ln\hat{A}) + \mathrm{i}\frac{N}{\sqrt{N_\mathrm{L}}}T^2\sum_{\mathrm{kk}'}\rho(-\mathrm{k})\lambda(\mathrm{k}'-\mathrm{k})\rho(\mathrm{k}) \\ & - \mathrm{i}q_0 N\sqrt{N_\mathrm{L}}\int \mathrm{d}\tau\lambda(\mathbf{0};\tau) - \frac{NU_\mathrm{fc}}{4}T\sum_\mathrm{k}\varphi^\mathrm{f}(\mathrm{k})\varphi^\mathrm{c}(-\mathrm{k}), \end{aligned} \tag{11}$$

where the abbreviation $\mathrm{k} = (\vec{k}, \mathrm{i}\omega_n)$, etc has been introduced and matrix $\hat{A}$ is defined as

$$A_{\mathrm{kk}'} = \begin{bmatrix} (-\mathrm{i}\omega_n + \epsilon_{\vec{k}})\delta_{\mathrm{kk}'} + \frac{U_\mathrm{fc}}{2\sqrt{N_\mathrm{L}}}T\varphi^\mathrm{f}(\mathrm{k}-\mathrm{k}') & T\frac{V}{\sqrt{N_\mathrm{L}}}\rho(\mathrm{k}-\mathrm{k}') \\ T\frac{V}{\sqrt{N_\mathrm{L}}}\rho^*(\mathrm{k}-\mathrm{k}') & (-\mathrm{i}\omega_n + \epsilon_\mathrm{f})\delta_{\mathrm{kk}'} + \frac{T}{\sqrt{N_\mathrm{L}}}\mathrm{i}\lambda(\mathrm{k}-\mathrm{k}') + \frac{TU_\mathrm{fc}}{2\sqrt{N_\mathrm{L}}}\varphi^\mathrm{c}(\mathrm{k}-\mathrm{k}') \end{bmatrix}. \tag{12}$$

With the use of the mean-field solution for ρ, λ, φ^f, and φ^c, which optimizes the action (11), the f-electron number (per 'spin'), $\bar{n}_\mathrm{f} \equiv n_\mathrm{f}/2$, as a function of ϵ_f, is given for a series of values of U_fc/D, D being the Fermi energy of the spherical conduction band, as shown in figure 6. Here we set the hybridization as $V = 0.5D$ and total electron number per 'spin' as $n \equiv \bar{n}_\mathrm{f} + \bar{n}_\mathrm{c} = 0.875$. We adopted the dispersion of conduction electrons $\epsilon_{\vec{k}} = k^2/2m - D$, where the bottom of the conduction band is set as $-D$, and assumed that the density of states $N_0(\epsilon)$ per conduction electron with particular 'spin' is given such that $\int_{-D}^{D}\mathrm{d}\epsilon N_0(\epsilon) = 1$.

These results are consistent with those of previous works [63–65], and also with a physical picture that the rapid valence change occurs at the condition (4) which is fulfilled in the case where the energies of f^0- and f^1 state are degenerate. For much larger values of U_fc or smaller values of V than those presented in figure 6, there occurs a first-order-like discontinuous transition although this is not shown there (see [66, 67]). In the mean-field level of approximation for the slave boson Hamiltonian, our treatment of the effect of U_fc is just like

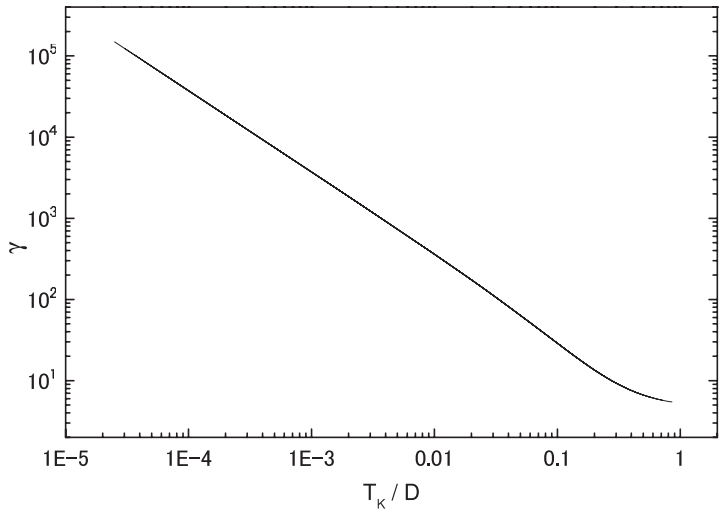

Figure 7. Sommerfeld constant γ versus Kondo temperature T_K, defined by $T_K = \bar{\epsilon}_f - \mu$. The parameters used are the same as those in figure 6. Results for different values of U_{fc}/D lie on the same line, exhibiting a universal behaviour.

that in the Hartree–Fock approximation [63–65]. It is noted that the valence change occurs more sharply if we estimate it in the much more appropriate approximation on the extended Gutzwiller variational wavefunction [66]. In this sense, the sharpness of the valence change may be underestimated by the present treatment.

Using the mean-field solution, $\bar{\rho}$, $\bar{\lambda}$, $\bar{\varphi}^f$, and $\bar{\varphi}^c$, the dispersion of quasiparticles is given as

$$E^{\pm}_{\vec{k}} = \tfrac{1}{2}[\bar{\epsilon}_f + \bar{\epsilon}_{\vec{k}} \pm \sqrt{(\bar{\epsilon}_f - \bar{\epsilon}_{\vec{k}})^2 + 4\bar{V}^2}], \tag{13}$$

where

$$\begin{aligned} \bar{\epsilon}_k &\equiv \epsilon_k + U_{fc}\bar{n}_f, \\ \bar{\epsilon}_f &\equiv \epsilon_f + i\bar{\lambda}/\sqrt{N_L} + U_{fc}\bar{n}_c, \\ \bar{V} &\equiv V\bar{\rho}/\sqrt{N_L}, \end{aligned} \tag{14}$$

where $\bar{n}_f \equiv \langle n_f \rangle_{MF}$, the f-electron numbers per site and 'spin', and $\bar{n}_c \equiv \langle n_c \rangle_{MF}$, the number of conduction electrons per site and 'spin'. Then, the density of states $\rho(\mu)$ of quasiparticles at the Fermi energy is calculated, and the Sommerfeld constant γ of the specific heat is given by the relation

$$\gamma = \frac{\pi^2}{3} D\rho(\mu)N, \tag{15}$$

where N (now $N = 2$) is the degeneracy of the quasiparticles. The so-called Kondo temperature, or the characteristic temperature, of the present model, is defined simply as $(\bar{\epsilon}_f - \mu)$. In figure 7, we can see that the relation $T_K \propto \gamma^{-1}$ holds rather nicely. It is remarked that the relation T_K versus γ with different values of U_{fc} are lying on a line exhibiting a kind of universality. It is suggested that the effect of U_{fc} can be absorbed into the other parameters of the conventional PAM at least at the mean-field level, as in the case of the single-impurity Anderson model. However, in the lattice case, the first-order-like transition occurs through the effects of U_{fc} even in the mean-field approximation. This is considered to be a distinctive effect of U_{fc} in the PAM.

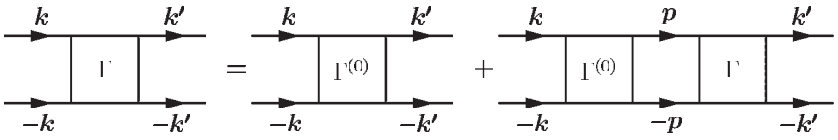

Figure 8. Feynman diagram representing the integral equations for the scattering amplitude of two quasiparticles Γ from $(\vec{k}, -\vec{k})$ to $(\vec{k}', -\vec{k}')$.

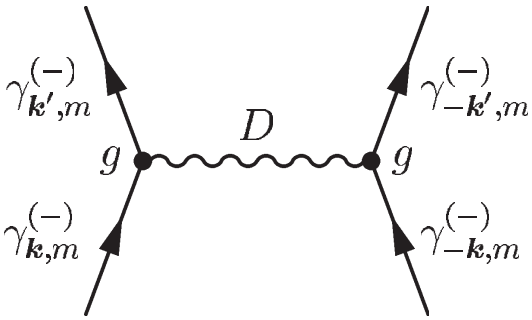

Figure 9. Feynman diagram for the irreducible vertex part $\Gamma^{(0)}$ to leading order in $1/N$. The explicit form of the fluctuation propagator D is given by equation (17) and its interaction vertex g with quasiparticles arises from the matrix $\hat{A}$ given by (12).

3.1.2. Superconducting transition temperature [34]. Next, a possible type of the superconducting gap is discussed near the region where the rapid valence change occurs owing to $U_{\rm fc}$, the f–c Coulomb interaction, in the extended periodic Anderson model. In the conventional PAM, problems of determining the superconducting transition temperature $T_{\rm c}$ have been studied by several authors within the slave-boson and $1/N$-expansion method [75, 76], in which the Gaussian fluctuations of relevant parameters around the mean-field solution. Following their method, here the Gaussian fluctuations of $\tilde{\rho} \equiv \rho - \bar{\rho}$, $\tilde{\lambda} \equiv \lambda - \bar{\lambda}$, $\tilde{\varphi}^{\rm f} \equiv \varphi^{\rm f} - \bar{\varphi}^{\rm f}$, and $\tilde{\varphi}^{\rm c} \equiv \varphi^{\rm c} - \bar{\varphi}^{\rm c}$, are taken into account. The $T_{\rm c}$ is obtained from the integral equation of the particle–particle scattering amplitude, Γ, for two quasiparticles with opposite momentum near the Fermi surface (see figure 8). The quasiparticle operators can be represented by a unitary transformation in terms of f- and conduction electron operators as

$$\begin{bmatrix} \gamma^{(+)}_{\vec{k}} \\ \gamma^{(-)}_{\vec{k}} \end{bmatrix} = \begin{bmatrix} u_{\vec{k}} & v_{\vec{k}} \\ -v_{\vec{k}} & u_{\vec{k}} \end{bmatrix} \begin{bmatrix} {\rm f}_{\vec{k}} \\ {\rm c}_{\vec{k}} \end{bmatrix}, \tag{16}$$

where $\gamma^{(\pm)}$ corresponds to the eigenvalues $E^{\pm}$, equation (13), respectively. The scattering amplitude Γ is obtained from the two-quasiparticle correlation function,

$$\langle {\rm T}_\tau \gamma^{(-)}_{\vec{k},m}(\tau_1)\gamma^{(-)}_{-\vec{k}',m'}(\tau_2)\gamma^{(-)\dagger}_{-\vec{k},m'}(\tau_3)\gamma^{(-)\dagger}_{\vec{k},m}(\tau_4)\rangle,$$

by removing the external legs.

To leading order in $1/N$, the irreducible vertex part $\Gamma^{(0)}$ includes only single-fluctuation exchange processes as shown in figure 9. With the use of relation (16), the analytic expression of $\Gamma^{(0)}$ is given as follows [34]:

$$\Gamma^{(0)} = v^4 \left\{ D_{\lambda\lambda} + \frac{U_{\rm fc}}{2} D_{\lambda\varphi^{\rm c}} + \frac{U_{\rm fc}}{2} D_{\varphi^{\rm c}\lambda} + \left(\frac{U_{\rm fc}}{2}\right)^2 D_{\varphi^{\rm c}\varphi^{\rm c}} \right\} - 4uv^3 \left\{ V D_{\lambda\rho} + \frac{U_{\rm fc}}{2} D_{\varphi^{\rm c}\rho} \right\}$$
$$+ u^2 v^2 \left[2 \left\{ \frac{U_{\rm fc}}{2} D_{\lambda\varphi^{\rm f}} + \left(\frac{U_{\rm fc}}{2}\right)^2 D_{\varphi^{\rm c}\varphi^{\rm f}} \right\} + 4V^2 D_{\rho\rho} \right]$$

$$- u^3 v 4V \frac{U_{\rm fc}}{2} D_{\varphi^{\rm f}\rho} + u^4 \left(\frac{U_{\rm fc}}{2}\right)^2 D_{\varphi^{\rm f}\varphi^{\rm f}}, \tag{17}$$

where fluctuation propagators Ds are defined as

$$D_{\alpha\beta}(\vec{k};\tau) \equiv -\langle {\rm T}_\tau \alpha(\vec{k},\tau)\beta^\dagger(\vec{k},0)\rangle, \tag{18}$$

where α, β are $\tilde{\rho}$, $\tilde{\lambda}$, $\tilde{\varphi}^{\rm f}$, $\tilde{\varphi}^{\rm c}$.

With the use of (17), $T_{\rm c}$ is calculated in the weak coupling theory in which the external momenta are set on the Fermi surface, i.e. $|\vec{k}|$, $|\vec{k}'| \to k_{\rm F}$, and the static limit, $\omega \to 0$, is taken in the boson propagators. Then, the linearized gap equation is represented by figure 8 Namely, the scattering amplitude is decomposed into the Legendre polynomial as

$$\Gamma(\vec{k},\vec{k}') = \sum_{\ell=0}^{\infty}(2\ell+1)\Gamma_\ell {\rm P}_\ell(\hat{\vec{k}}\cdot\hat{\vec{k}}'). \tag{19}$$

The scattering amplitude Γ_ℓ corresponding to the channel with relative angular momentum ℓ is given by

$$\Gamma_\ell = \frac{\Gamma_\ell^{(0)}}{1+\rho(\mu)\Gamma_\ell^{(0)}\ln(\frac{T_{\rm K}}{T})}, \tag{20}$$

where the $\Gamma_\ell^{(0)}$ are related to the $\Gamma^{(0)}(\hat{\vec{k}}\cdot\hat{\vec{k}}')$ by the formula

$$\Gamma_\ell^{(0)} = \tfrac{1}{2}\int_{-1}^{1} {\rm d}(\cos\theta)\Gamma^{(0)}(\theta){\rm P}_l(\cos\theta). \tag{21}$$

Then the transition temperature $T_{\rm c}$ for the ℓ-wave channel is given by

$$T_{\rm c} = T_{\rm K}\exp\left[\frac{1}{\rho(\mu)\Gamma_\ell^{(0)}}\right]. \tag{22}$$

Here it is noted that the energy cut-off, corresponding to the Debye frequency, is given by $T_{\rm K} \equiv \bar{\epsilon}_{\rm f} - \mu$, the bandwidth of the quasiparticles.

A non-negligible $T_{\rm c}$ is obtained for the d-wave ($\ell = 2$) channel as far as the channels $\ell = 0$, 1 and 2, are concerned. The results of $T_{\rm c}$ versus $\epsilon_{\rm f}$ are shown in figure 6 for a series of values of $U_{\rm fc}$, the repulsion between f and conduction electrons. There exists a sharp peak of $T_{\rm c}$ at around $\epsilon_{\rm f}$ where $n_{\rm f}$ starts to show a rapid decrease. Its tendency becomes more drastic as $U_{\rm fc}$ increases, making the valence change sharper. In the region where the f-electron number is decreased enough, $T_{\rm c}$ is strongly suppressed.

It can be analysed which term in equation (17) plays an important role for the pairing interaction. As seen in figure 10, it turned out that the major part of $\Gamma^{(0)}(q)$ ($=V_{\mathbf{k},\mathbf{k}'}$ with $\mathbf{q} = \mathbf{k} - \mathbf{k}'$) is induced by the scattering process (f, f) $\to$ (f, c) or (f, c) $\to$ (f, f), in which the valence of f electrons is changed directly. Here it is remarked that the pairing interaction $\Gamma^{(0)}(q)$ is almost q independent up to $q < 3k_{\rm F}/2$, reflecting the local nature of CVF, while the dimensionless coupling $\Gamma^{(0)}(q)\rho(0)$ at the Fermi level is greatly enhanced near the CVT point. It is this locality that is the origin of d-wave pairing as in the case of two-dimensional isotropic Fermi liquid near the magnetic phase boundary [78]. Namely, the q-independent part of $\Gamma^{(0)}$ gives a short range repulsion of the s-wave component, while the decrement (at $q > (3/2)k_{\rm F}$) from the q-independent part gives us an attractive component with large wavenumber transfer of $\mathcal{O}(2k_{\rm F})$, promoting the pairing with higher angular momentum, d wave in the present case. This locality should be maintained for the case where the conduction band is subject to the effect of lattice periodicity. In the latter case, the attractive interaction works among quasiparticles located at adjacent sites and p- or d- or f-wave-like pairing is induced

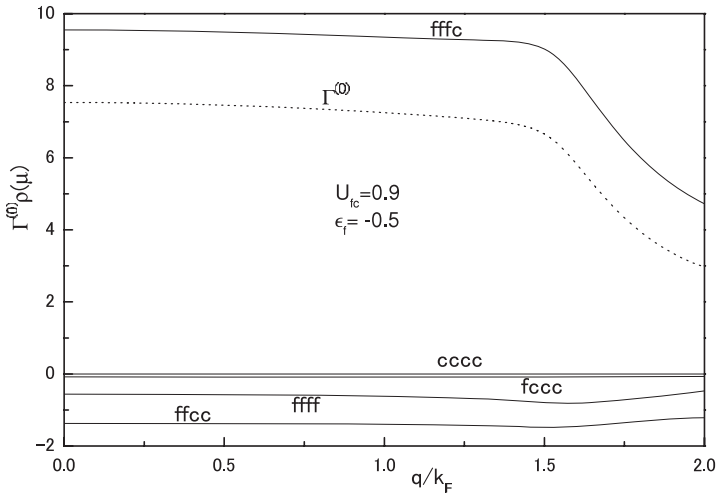

Figure 10. $\Gamma^{(0)}(q)$ as a function of momentum transfer q for each scattering channel included in equation (17). For example, 'ffff' means the v^4 term of equation (17). The others are represented similarly.

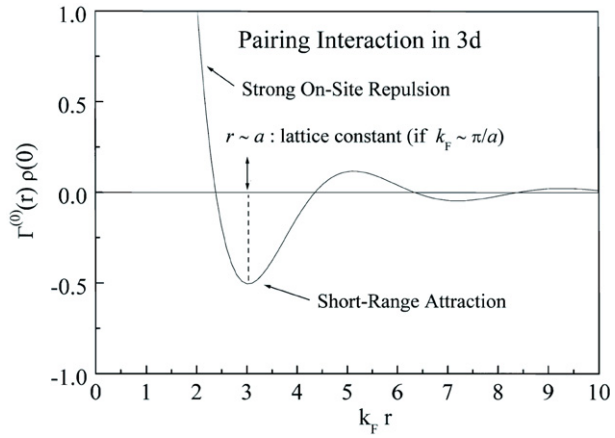

Figure 11. Real-space pairing interaction $\Gamma^0(r)\rho(0)$. The parameter set adopted is the same as that in figure 10.

depending on the shape of the Fermi surface because the attraction due to CVF does not have 'spin' dependence, unlike the spin-fluctuation mechanism [4, 79].

The reason for the d-wave pairing can be seen more clearly by inspecting a real space picture of the pairing interaction

$$\Gamma^0(r) = \sum_{\mathbf{q}} \Gamma^0(q) \mathrm{e}^{\mathrm{i}\mathbf{q}\cdot\mathbf{r}}. \tag{23}$$

The result for $\Gamma^0(r)$ is shown in figure 11 for the same parameter set as figure 10. This clearly shows the existence of the extended attraction together with the one-site strong repulsion. If we assume $k_\mathrm{F} \sim \pi/a$, a being the lattice constant as in typical metals, the attraction works between the nearest neighbour sites. Then, according to the discussion in section 1, the d-wave

pairing is promoted. The p-wave 'spin-triplet' pairing is also possible in principle in this case because the attraction mediated by the valence fluctuation has no spin dependence.

3.2. Physical picture of critical-valence–fluctuation mechanism [37]

The physical interpretation of the present valence fluctuation mediated pairing interaction is given as follows. A clue comes from the local nature of the interaction, and the prediction of d-wave pairing symmetry, which together imply nearest-neighbour pairing. One can imagine a largely filled f band, with each filled f^1 site experiencing a Coulomb repulsion U_{cf} with the respective conduction (c-) electrons. As the pressure is increased and ϵ_f moves closer to the Fermi level ϵ_F, there will come a point where $\epsilon_f + U_{cf}\langle n_c\rangle = E_F$ and the f band will start to empty. On an individual $4f^0$ 'hole' site, the U_{cf} interaction will be absent, thus an increased density of conduction electrons would be energetically favourable at this position. If this extra 'screening' conduction electron density is not strictly localized onto the atom itself, but spreads onto neighbouring sites, the f electrons on Ce atoms around the original 'hole' site will feel an increased repulsion. The tendency to transfer electrons from the f to conduction bands will be locally reinforced, explaining intuitively the increasingly catastrophic drop in n_f for larger U_{cf}, predicted in [34]. For large enough U_{cf}, phase separation would be expected to occur for some values of ϵ_f.

The attractive pairing interaction can be explained as follows: consider an isolated pair of $4f^0$ 'holes', accompanied by their cloud of conduction electrons. If these are separated by two lattice positions, with an intervening filled $4f^1$ site, the two clouds of conduction electrons will overlap at the intermediate site, further increasing the Coulomb energy at that point. It would therefore be energetically favourable for the two 'holes' to be on neighbouring atoms, thus with attractive interaction. The attractive interaction between 'holes' is equivalent to that between 'electrons', so that this argument would give an intuitive understanding of the origin of the valence–fluctuation mechanism of superconductivity.

In the Kondo regime where $n_f \approx 1$ ($\bar{n}_f \approx 1/2$), the spin fluctuations are believed to play the most important role for the occurrence of superconductivity. In such a region we have to take into account the higher order term beyond $1/N$ to discuss the instability to the superconducting state, since the spin-fluctuation contribution to the effective interaction appears only beyond at the order $(1/N)^2$ [76]. However, the present approach of the order of $1/N$ is still expected to work in the region where the valence fluctuations play an important role.

3.3. Valence fluctuations versus orbital fluctuations

There exist a few viewpoints different from ours for explaining the anomalous properties of $CeCu_2Ge_2$. One of them is to attribute its origin to the orbital fluctuations in the multiband periodic Anderson model, in which the broad bandwidth under high pressure is expected to change the degeneracy of the f-electron state. Indeed, this has been proposed in [30], paying attention to the fact that, at the pressure corresponding to the peak of T_c and ρ_0, the two temperatures T_1^{max} and T_2^{max} at which the resistivity peaks merge with each other, indicating the Kondo temperature becomes of the order of the crystalline electric field (CEF) splitting. The orbital fluctuation mechanism has also been proposed as a possible mechanism for explaining the phenomena observed in $CeCu_2Ge_2$, and discussing that the orbital fluctuation is enhanced where T_K is comparable to CEF splitting [80]. The effect of orbital fluctuations on the spin-fluctuation mechanism has also been studied as a model of Ce115 systems [81].

However, the merging of T_1^{max} and T_2^{max} seems to be a general feature at P_v in compounds where a critical valence transition is thought to exist. This can be understood as follows.

First of all, the so-called Kondo temperature $T_{\rm K}$, related to $T_i^{\rm max}$ $(i = 1, 2)$, depends crucially on the degeneracy $(2\ell+1)$ of the local f state: $T_{\rm K} \sim D\exp[-1/(2\ell+1)\rho_{\rm F}|J|]$, where D is the bandwidth of conduction electrons, $\rho_{\rm F}$ the density of states of conduction electrons at the Fermi level, and J the c–f exchange coupling constant [82]. Even though the sixfold degeneracy of the local 4f state is lifted by the CEF effect, leaving the Kramers doublet ground state with the excited CEF levels with excitation energy $\Delta_{\rm CEF}$, the Kondo temperature $T_{\rm K}$ is still enhanced considerably by the effect of the excited CEF level [83].

Secondly, the technical degeneracy of CEF levels, relevant to the Kondo effect, is affected by the broadening ΔE of the lowest CEF level. If $\Delta E \ll \Delta_{\rm CEF}$, the degeneracy relevant to $T_{\rm K}$ is twofold. On the other hand, if $\Delta E > \Delta_{\rm CEF}$, it increases to four- or sixfold. The level broadening is given by $\Delta E \simeq z\pi\rho_{\rm F}|V|^2$, where $|V|$ is the strength of c–f hybridization, and z is the renormalization factor, which gives the inverse of mass enhancement in the case of the lattice system. It is crucial that ΔE is very sensitive to the valence of the Ce ion because z is essentially given by equation (1). In particular, the factor z increases from the tiny value in the Kondo regime, $z \sim (1 - n_{\rm f}) \ll 1$, and approaches unity in the so-called valence fluctuation regime.

Since the factor $\pi\rho_{\rm F}|V|^2 \gg \Delta_{\rm CEF}$ in general for Ce-based heavy electron systems, the ratio $\Delta E/\Delta_{\rm CEF}$, which is much smaller than unity in the Kondo regime, greatly exceeds unity across the valence transformation around $P \sim P_{\rm v}$, leading to the increase of the technical degeneracy of the f state, *irrespective of a sharpness of the valence transformation*. Therefore, $T_1^{\rm max}$ should merge with $T_2^{\rm max}$, which corresponds to four- or sixfold degeneracy of the 4f state due to the effect of finite temperature, i.e. $T \sim \Delta_{\rm CEF}$. This may be the reason why $T_1^{\rm max}$ increases and approaches $T_2^{\rm max}$ at pressure where $T_{\rm c}$ exhibits the maximum, or the KW ratio changes between strongly and weakly correlated classes. This general behaviour has recently been verified by a microscopic calculation on the basis of the multiorbital PAM with CEF splitting [84].

3.4. T-linear resistivity and enhanced Sommerfeld coefficient at $P = P_{\rm v}$ [37]

The T-linear temperature dependence of the resistivity observed in a narrow pressure region around $P \sim P_{\rm v}$ is understood in the following discussions. The origin of d-wave superconductivity induced by CVF is the locality of pairing interaction as discussed in a previous section. Namely, the static limit of the effective interaction $\Gamma^{(0)}(q, {\rm i}\omega_m)$ between quasiparticles is enhanced greatly around $P \sim P_{\rm v}$, and is almost independent of q, the momentum transfer, up to $\sim 3/2$ of $p_{\rm F}$. This must be due to the local nature of the CVF, whose response function, $\chi_{\rm v}(q, \omega)$, is also almost q independent in the low frequency region. On this observation, we present here a semi-phenomenological theory explaining the T-linear resistivity and the enhancement of the Sommerfeld coefficient γ around $P \sim P_{\rm v}$. A microscopic origin of the locality will be discussed in section 4.

We adopt an exponentially decaying phenomenological form for the valence–fluctuation propagator (dynamical valence susceptibility) $\chi_{\rm v}$:

$$\chi_{\rm v}(q, \omega) \equiv {\rm i}\int_0^\infty {\rm d}t {\rm e}^{{\rm i}\omega t}\langle[n_{\rm f}(q, t), n_{\rm f}(-q, 0)]\rangle \tag{24}$$

$$= \frac{K}{\omega_{\rm v} - {\rm i}\omega}, \qquad \text{for } q < q_{\rm c} \sim p_{\rm F} \tag{25}$$

where $n_{\rm f}(q)$ is the Fourier component of the number of f electrons per Ce site, K is a constant of $\mathcal{O}(1)$ and the parameter $\omega_{\rm v}$ parameterizes the closeness to criticality. $\omega_{\rm v}$ is inversely proportional to the valence susceptibility $\chi_{\rm v}(0, 0) = -(\partial n_{\rm f}/\partial\epsilon_{\rm f})_\mu$, $\epsilon_{\rm f}$ being the atomic level of the f electron of the Ce ion, and μ the chemical potential.

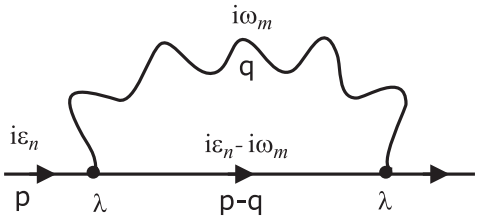

Figure 12. Feynman diagram for the self-energy due to the one-fluctuation mode exchange process. λ denotes the coupling between the valence–fluctuation mode and the quasiparticles.

The retarded self-energy $\Sigma^{\mathrm{R}}_{\mathrm{vf}}(p, \epsilon + \mathrm{i}\delta)$ gives a measure of the quasiparticle effective mass and lifetime respectively in its real and imaginary parts. The explicit form of $\Sigma^{\mathrm{R}}_{\mathrm{vf}}(p, \epsilon + \mathrm{i}\delta)$ corresponding to the Feynman diagram figure 12 can be calculated in a standard way.

In typical limiting cases, $\mathrm{Im}\,\Sigma^{\mathrm{R}}_{\mathrm{vf}}(p_{\mathrm{F}}, \epsilon)$ can be straightforwardly calculated in the approximation on the dispersion of the quasiparticles, $\xi_{\mathbf{p}-\mathbf{q}} \simeq -vq\cos\theta$, where θ is the angle between $\mathbf{p}$ and $\mathbf{q}$, v is the quasiparticle velocity and p is assumed to be on the Fermi surface, i.e., $p = p_{\mathrm{F}}$.

$T = 0, \epsilon \neq 0$:

$$\mathrm{Im}\,\Sigma^{\mathrm{R}}_{\mathrm{vf}}(p_{\mathrm{F}}, \epsilon) \simeq -\frac{|\lambda|^2 K q_{\mathrm{c}}^2}{32\pi^2 v} \ln\left(1 + \frac{\epsilon^2}{\omega_{\mathrm{v}}^2}\right), \tag{26}$$

where q_{c} is the cut-off wavenumber of the order of k_{F}.

$\epsilon = 0, 0 < T \ll \epsilon_{\mathrm{F}}$:

$$\mathrm{Im}\,\Sigma^{\mathrm{R}}_{\mathrm{vf}}(p_{\mathrm{F}}, 0) \simeq -\frac{|\lambda|^2 K q_{\mathrm{c}}^2}{4\pi^2 v}\frac{T}{\omega_{\mathrm{v}}}\tan^{-1}\frac{T}{\omega_{\mathrm{v}}} \simeq -\frac{|\lambda|^2 K q_{\mathrm{c}}^2}{4\pi^2 v}\begin{cases}\left(\dfrac{T}{\omega_{\mathrm{v}}}\right)^2, & T \ll \omega_{\mathrm{v}} \\ \dfrac{\pi}{2}\dfrac{T}{\omega_{\mathrm{v}}}, & T \gg \omega_{\mathrm{v}}.\end{cases} \tag{27}$$

The latter result, $\mathrm{Im}\,\Sigma_{\mathrm{vf}}(p_{\mathrm{F}}, \epsilon = 0) \propto T/\omega_{\mathrm{v}}$ for $T \gg \omega_{\mathrm{v}}$, implies that almost all the critical valence–fluctuation modes can be regarded as classical at $T > \omega_{\mathrm{v}}$, and T-linear dependence stems from the asymptotic form of the Bose distribution function $g(\omega) = 1/(\mathrm{e}^{\omega/T} - 1) \simeq T/\omega$.

In the limit $\omega_{\mathrm{v}} \ll vp_{\mathrm{F}}$, the real part of the self-energy, shown in figure 12, can be also calculated easily at $T = 0$ and $\epsilon \sim 0$, leading to

$$\mathrm{Re}\,\Sigma^{\mathrm{R}}_{\mathrm{vf}}(p_{\mathrm{F}}, \epsilon) \simeq -\frac{|\lambda|^2 K q_{\mathrm{c}}^2}{2\pi^2 v}\frac{\epsilon}{\omega_{\mathrm{v}}}\int_0^1 \mathrm{d}u \frac{1-u^2}{u^2+1}\ln\left|\frac{1}{u}\right| \tag{28}$$

$$\propto -\frac{\epsilon}{\omega_{\mathrm{v}}}, \tag{29}$$

where $u = vqt/\omega_{\mathrm{v}}$.

The T-linear dependence of $\mathrm{Im}\,\Sigma^{\mathrm{R}}_{\mathrm{vf}}(p, 0)$, for $T > \omega_{\mathrm{v}}$, (27), implies T-linear resistivity, as the quasiparticles are subject to the large angle scattering by the critical valence–fluctuation modes. These are effective in a wide region in the Brillouin zone due to their local nature and easily couple to the Umklapp process of quasiparticle scattering. This result is consistent with the experimental fact that T-linear resistivity is observed in a narrow pressure region around P_{v} which is considered to correspond to the nearly critical transition of the valence of the Ce ion.

Such a T-linear dependence has been discussed in the context of high-T_{c} cuprates with a marginal Fermi liquid (MFL) assumption, [85] and charge transfer fluctuations were once considered as an origin for MFL [85, 86], while further theoretical models have been put forth up to now [87]. Excepting the T-linear resistivity, the present result is different from MFL

behaviour. The self-energy exhibits different energy dependence, while the idea for the origin of our singular behaviour shares aspects similar to the first idea of a charge transfer mechanism for high-T_c cuprates [68, 86]. $\Sigma(\epsilon)$ in the MFL model is given as $\Sigma(\epsilon) \propto (\epsilon \ln \epsilon - i|\epsilon|)$ [85], which is indeed different from the present case (equations (26) and (29)). In any case, it is to be noted that T-linear resistivity is accompanied by the peak of T_c in both systems, high-T_c cuprates and $CeCu_2Si_2$.

The result (29) implies that the mass enhancement $(1 - \partial \mathrm{Re}\Sigma^{\mathrm{R}}_{\mathrm{vf}}(\epsilon)/\partial\epsilon)$ is expected around $P \sim P_v$. Namely, the effective mass is given by

$$m^* \propto \bar{m}\frac{1}{\omega_v}, \tag{30}$$

where $\bar{m}$ is the effective mass renormalized by the conventional correlation effect, leading to heavy electrons, i.e. not including the effect of CVF. This latter effective mass $\bar{m}$ exhibits a drastic decrease around $P \sim P_v$, while the second factor of (30) is enhanced. Both effects should be reflected in the Sommerfeld coefficient γ, so that the peak of $\gamma \propto m^*$ is shifted to the lower pressure (larger $\bar{m}$) side, and the anomaly of γ due to the valence fluctuations may be smeared to some extent. Nevertheless, some trace should be observed. (The shift of the peak of γ can be understood as the superposition of the two trends using a model P-dependence of $\bar{m}$ and ω_v.) Indeed, the experimental result presented in figure 4 may be explained by this effect. A similar trend has been reported in a series of solid solutions of Ce-based intermetallic compounds [88].

3.5. Enhanced residual resistivity [35]

The effect of CVF on impurity scattering can be considered in the context of the many-body renormalization effect of the impurity potential in general [52, 89–94]. More than three decades ago, Betbeder-Matibet and Nozières [89] showed on the basis of the Ward–Pitaevskii identity that the impurity potential, in a one-component Fermi liquid, is renormalized in the forward scattering limit as

$$\tilde{u}(\vec{k} \to 0) = \frac{1}{z(1 + F_0^s)} u(\vec{k} \to 0), \tag{31}$$

where $u(\vec{k})$ is the bare nonmagnetic impurity potential and $\tilde{u}(\vec{k})$ is the renormalized one, z is the renormalization amplitude including *all* of the many-body effects and F_0^s is the Landau parameter relevant to the correction of the charge susceptibility. Relation (31) implies that the forward impurity scattering is renormalized in proportion to the charge susceptibility $\chi_{\mathrm{charge}} = z^{-1}(2N_F)/(1 + F_0^s)$. Recently, it was shown [35] that a similar relation holds for the impurity scattering of f electrons in the two-component Fermi liquid described by the Hamiltonian (3):

$$\tilde{u}(\vec{k} \to 0) \approx -\frac{1}{2N_F}\left(\frac{\partial n_f}{\partial \epsilon_f}\right)_\mu u(\vec{k} \to 0), \tag{32}$$

where n_f is the f-electron number density and N_F is the density of states of noninteracting electrons described by (3) at the Fermi level. This is an analogue of relation (31), in which the factor $1/z(1 + F_0^s)$ is re-expressed as $\chi_{\mathrm{charge}}/N_F$. The relation (32) implies that the impurity scattering is critically enhanced if the valence of the Ce ion changes critically when the f level ϵ_f is tuned, relative to the Fermi level, by the pressure.

Let us recapitulate the derivation of the relation (32). We start with the model Hamiltonian (3). The one-particle Green function for a given spin direction in this system

is given formally as

$$\left[G_{ij}^{-1}(\vec{p},\varepsilon)\right] = \begin{bmatrix} G_{\rm ff}(\vec{p},\varepsilon) & G_{\rm fc}(\vec{p},\varepsilon) \\ G_{\rm cf}(\vec{p},\varepsilon) & G_{\rm cc}(\vec{p},\varepsilon) \end{bmatrix}^{-1} \tag{33}$$

$$= \begin{bmatrix} \varepsilon - \epsilon_{\rm f} + \mu - \Sigma_{\rm ff}(\vec{p},\varepsilon) & -V_p - \Sigma_{\rm fc}(\vec{p},\varepsilon) \\ -V_p^* - \Sigma_{\rm cf}(\vec{p},\varepsilon) & \varepsilon - \xi_{\vec{p}} - \Sigma_{\rm cc}(\vec{p},\varepsilon) \end{bmatrix}, \tag{34}$$

where $\Sigma_{\rm ff}$ is the self-energy of the f electron and there also exist $\Sigma_{\rm fc}$ and $\Sigma_{\rm cc}$ as the many-body effect due to $U_{\rm ff}$ and $U_{\rm fc}$. It is noted that G_{ij}^{-1} represents the ij-element of the inverse matrix of the Green function, e.g. $G_{11}^{-1} \neq G_{\rm ff}^{-1}$ while $G_{11} = G_{\rm ff}$.

For coupling to nonmagnetic impurities, the scattering matrix for this system is given generally as $u_{ij}(\vec{k}) = \sum_{a=1}^{4} u_a(\vec{k})\lambda_{ij}^a$, where u_1 and u_2 are the variations of potential on f electrons and c electrons, respectively, while u_3 and u_4 represent the strength of the f–c mixing scattering. Here, λ_{ij}^a is the bare vertex for coupling to impurities and is given by $[\lambda_{ij}^1] = (1+\tau^z)/2$, $[\lambda_{ij}^2] = (1-\tau^z)/2$, $[\lambda_{ij}^3] = \tau^x/\sqrt{2}$ and $[\lambda_{ij}^4] = \tau^y/\sqrt{2}$, with $\vec{\tau}$ being the Pauli matrices in the f–c space.

In the following, a Greek index, α, represents the dependence on both the component $i = 1, 2$ and the spin $\sigma = \ \uparrow, \downarrow$, and the summation is assumed to be for repeated indices. Then, the one-particle Green function and the scattering matrix mean the tensor product multiplied by the unit matrix with respect to the spin variables.

The Ward–Pitaevskii identity relevant to the present problem is given considering the linear response of $G_{\gamma\alpha}$ caused by the shift of the parameter, denoted by ϵ_a, with the chemical potential μ being fixed. Here, ϵ_a is the f level $\epsilon_{\rm f}$, the centre of the conduction band $\epsilon_{\rm c}$ or f–c mixing V, i.e., ${}^t[\epsilon_a] = (\epsilon_1, \epsilon_2, \epsilon_3, \epsilon_4) = (\epsilon_{\rm f}, \epsilon_{\rm c}, \sqrt{2}V', \sqrt{2}V'')$, with V' and V'' being the real and imaginary parts of V, respectively. One can show, by analysing the structure of the perturbation series of the self-energy, that the following identity holds [95]:

$$-\left(\frac{\partial G_{\gamma\alpha}^{-1}(p)}{\partial \epsilon_a}\right)_\mu = \lambda_{\gamma\alpha}^a + \left(\frac{\partial \Sigma_{\gamma\alpha}(p)}{\partial \epsilon_a}\right)_\mu \tag{35}$$

$$= \lambda_{\gamma\alpha}^a - {\rm i}\int \frac{{\rm d}^4 q}{(2\pi)^4} \Gamma_{\gamma\delta,\alpha\beta}^k(p,q)\{G_{\beta\zeta}(q)G_{\kappa\delta}(q)\}_k, \lambda_{\zeta\kappa}^a, \tag{36}$$

where Γ^k is the so-called k-limit of the full vertex function, and $\{GG\}_k$ is that of the particle–hole Green function pair with the four-vector abbreviations $p = (\vec{p}, \varepsilon)$, etc. The process of the renormalization of impurity potential is represented by the Feynman diagram, as shown in figure 13. In the limit of forward scattering, i.e. $k \to 0$, the renormalized potential $\tilde{u}_a(\vec{k})$ and the bare one $u_a(\vec{k})$ are in the relation

$$\lim_{k\to 0} \tilde{u}_a(\vec{k}) = \lim_{k\to 0} \tfrac{1}{2}\lambda_{\alpha\gamma}^a u_b(\vec{k}) \times \left[\lambda_{\gamma\alpha}^b - {\rm i}\int \frac{{\rm d}^4 q}{(2\pi)^4} \Gamma_{\gamma\delta,\alpha\beta}^k(p,q)\{G_{\beta\zeta}(q)G_{\kappa\delta}(q)\}_k \lambda_{\zeta\kappa}^b\right]. \tag{37}$$

The reason why the k-limit vertex appears in (37) is that the impurity scattering is elastic, maintaining the energy transfer $\omega = 0$. Therefore, on the basis of relation (36), the impurity potential is renormalized by $-(\partial G_{\gamma\alpha}^{-1}(\vec{p},\varepsilon)/\partial\epsilon_a)_\mu$ in the limit $k \to 0$.

In heavy electrons, the important effect of the impurity on the the quasiparticles arises from the variations of potential on f electrons, because the quasiparticles consist mainly of f electrons. Of such effects, those due to the displacement of non-f elements from the regular alignment around Ce ions are subject to remarkable renormalization by the CVF, because the impurity potential due to such effects is under the unitarity limit and has potential for further

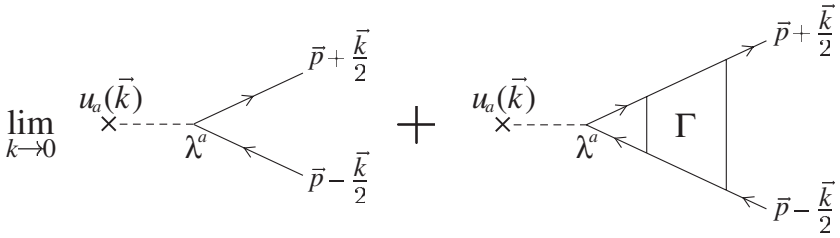

Figure 13. Feynman diagram for the exact vertex correction of impurity potential $u(\vec{k})$.

renormalization. On the other hand, the defect of Ce ions gives rise to the unitarity scattering from the beginning in the heavy electron state so that its potential is only subject to a gradual renormalization with a weak anomaly around a possible transition point from the Kondo regime to the VF regime. It is noted that even if we consider only the effect of the shift of the f level, i.e. in the case of $u_2 = u_3 = u_4 = 0$, the many-body effect due to $U_{\rm fc}$ gives rise to effective f–c and c–c scattering, as can be seen in (37).

In the case of heavy fermions whose quasiparticles consist mainly of f electrons, the relations (36) and (37) are simplified in such a way that the renormalization of the impurity potential is given essentially through f-electron scattering:

$$\lim_{k\to 0}\tilde{u}(\vec{k}) = -\lim_{k\to 0}u(\vec{k}) \times \frac{\partial}{\partial\epsilon_{\rm f}}G_{\rm ff}^{-1}(p,\varepsilon)\bigg|_{\mu}. \tag{38}$$

The derivatives in (38) are shown to be given by

$$\frac{\partial}{\partial\epsilon_{\rm f}}G_{\rm ff}^{-1}(p,\varepsilon)\bigg|_{\mu} \approx \left(\frac{1}{N_{\rm F}}\frac{\partial n_{\rm f}}{\partial\epsilon_{\rm f}}\right)_{\mu}. \tag{39}$$

Then the relation (32) results, implying that the impurity scattering is critically enhanced if the valence of the Ce ion changes critically when the f level $\epsilon_{\rm f}$ is tuned by pressure. Indeed, it happens to be the case as shown theoretically in section 3.1 that the derivative $-(\partial n_{\rm f}/\partial\epsilon_{\rm f})_n$ can diverge in the system described by the model Hamiltonian (3) with appropriate values of $U_{\rm fc}$ and $\epsilon_{\rm f}$. This means $-(\partial n_{\rm f}/\partial\epsilon_{\rm f})_\mu$ also diverges there, because the following relation holds, up to the approximation (39):

$$\left(\frac{\partial n_{\rm f}}{\partial\epsilon_{\rm f}}\right)_{\mu} \approx \frac{\left(\frac{\partial n_{\rm f}}{\partial\epsilon_{\rm f}}\right)_n}{1-\left(\frac{\partial n_{\rm f}}{\partial n}\right)_{\epsilon_{\rm f}}}, \tag{40}$$

where the derivative $-(\partial n_{\rm f}/\partial n)_{\epsilon_{\rm f}}$ is a small number of the order of z, the renormalization amplitude.

In order to see how this enhancement of the impurity potential affects the behaviour of the resistivity, we need to determine the k-dependence of $\tilde{u}(k)$ for scattering from $\vec{p}-\vec{k}/2$ to $\vec{p}+\vec{k}/2$ near the Fermi surface. Although generally it is not easy to determine the k-dependence accurately, it may be reasonable to parameterize it as

$$\tilde{u}(\vec{k}) \approx \frac{1}{\eta + Ak^2}u(\vec{k}), \tag{41}$$

where η is the inverse valence susceptibility, $\eta^{-1} \equiv |(\partial n_{\rm f}/\partial\epsilon_{\rm f})_\mu|/N_{\rm F}$, and $Ak_{\rm F}^2 \sim \mathcal{O}(1)$. As mentioned above there are two kinds of impurity potential for f electrons. One is due to the disorder of non-f elements and the other is due to the defect of Ce ions. The former gives

essentially the Born scattering, while the latter causes the scattering in the unitarity limit. Then the residual resistivity is expressed as

$$\rho_0 = \rho_0^{\rm Born} + \rho_0^{\rm unit}, \tag{42}$$

where $\rho_0^{\rm Born}$ is subject to huge enhancement by the CVF and $\rho_0^{\rm unit}$ is essentially unaffected. Indeed, $\rho_0^{\rm Born}$ is given as

$$\rho_0 \approx c_{\rm imp}\left\langle \frac{2\pi N_{\rm F}|u(\vec{k})|^2(1-\cos\theta)}{\left[\eta + A\left(2k_{\rm F}\sin(\theta/2)\right)^2\right]^2}\right\rangle_{\rm FS}, \tag{43}$$

where $c_{\rm imp}$ is the concentration of the impurity, θ is the angle between $\vec{p}\pm\vec{k}/2$, and the on-shell condition $\epsilon = \xi_{\vec{p}\pm\vec{k}/2} = 0$ has been used. $\langle\cdots\rangle_{\rm FS}$ means that the average with respect to $\vec{p}$ over the Fermi surface is taken. Here, it is noted that an explicit dependence of the renormalization amplitude does not appear due to cancellation between that for DOS and that for the damping rate of quasiparticles [96]. Calculation of the angular average over θ is performed easily, giving

$$\rho_0^{\rm Born} \propto c_{\rm imp}\ln\frac{1}{\eta}. \tag{44}$$

This result remains valid even if we take into account higher order terms by calculating the t-matrix. This is because the scattering by the renormalized potential (41) is merely the Rutherford scattering in the limit of $\eta \to 0$.

It should be noted that the present result is not contradictory to the Friedel sum rule according to which the scattering probability does not diverge as long as the extra charge accumulated locally around the impurity is finite [97, 98]. The form of the renormalized impurity potential (41) becomes long ranged as $\eta \to 0$ even though the bare potential is short ranged. Namely, the change of the valence near the impurity site extends over a long range in proportion to $1/r$, r being the distance from the impurity site as shown in figure 3(b). As a result, the total amount of valence change around the impurity from that of the host metal is divergent while the local charge of f and conduction electrons remains finite. Therefore, the effect of impurity becomes long ranged, making the scattering probability divergent.

Then, (42) is expressed as

$$\rho_0 = Bc_{\rm imp}|u(0)|^2\ln\left|\left(-\frac{\partial n_{\rm f}}{\partial\epsilon_{\rm f}}\right)_\mu \Big/ N_{\rm F}\right| + \rho_0^{\rm unit} \tag{45}$$

where the coefficient B depends on the band structure of host metals. The first term of (45) exhibits huge enhancement at the CVT point where $|(\partial n_{\rm f}/\partial\epsilon_{\rm f})_\mu|$ diverges. The expression (45) explains not only the huge enhancement of ρ_0 observed in $CeCu_2Si_2$ and $CeCu_2Ge_2$ at $P \simeq P_{\rm v}$ but also the universal behaviour of $\rho_0(P)$ for a bunch of samples with different qualities of crystals [37]. This huge enhancement should be compared to the moderate enhancement around the magnetic quantum critical point where the enhancement arises only through the renormalization amplitude z, as discussed in [52].

Quite recently, variation of $n_{\rm f}$ for a series of concentration x was measured by XAS in $EuCu_2(Ge_{1-x}Si_x)_2$, showing rapid change of $n_{\rm f}$ at $x \simeq 0.7$ [99]. Making use of an empirical relation relation of P–x, $\eta \propto (-\partial n_{\rm f}/\partial P)(\partial P/\partial\epsilon_{\rm f})$ was estimated, and then it turned out that the enhancement of the residual resistivity ρ_0 around $P = P_{\rm v}$ ($x = 0.7$) can be explained semiquantitatively by relation (44). Of course, in order to discuss the case of the Eu ion with the $4f^6$–$4f^7$ configuration, the model (3) has to be extended to the multiorbital case.

4. Locality of quantum critical valence transition

In this section, the reason for the locality of CVF in Ce-based heavy-fermion results is explained in semi-qualitative discussion. The universality class of CVF is expected to belong to that of the Gaussian fixed point while the wavenumber dependence of the valence susceptibility $\chi_{\rm v}$ is extremely weak [100]. It is remarked that there exists a crossover temperature T_x above which the dynamical exponent z is $z = \infty$, while $z = 3$ [33] in the low temperature limit $T \ll T_x$. In any case, the condition of the Gaussian fixed point, $d + z > 4$, is fulfilled. (There exists a cubic term with respect to the order parameter in general in the present problem. However, it is shown that the cubic term is marginally irrelevant in the case $d = 3$ and $z = 3$ [101].) Then, the estimation of $\chi_{\rm v}$ based on RPA can give us a clue to clarify its behaviour [102]. Due to the c–f hybridization, the enhancement of $\chi_{\rm v}$ is given as

$$\chi_{\rm v}(q, {\rm i}\omega_m) \sim \frac{\chi_{\rm cf}^{(0)}(q, {\rm i}\omega_m)}{1 - U_{\rm fc}\chi_{\rm cf}^{(0)}(q, {\rm i}\omega_m)} \tag{46}$$

where $\chi_{\rm cf}^{(0)}(q, {\rm i}\omega_m)$ is defined as follows:

$$\chi_{\rm cf}^{(0)}(q, {\rm i}\omega_m) \equiv -T \sum_n \sum_{\vec{p}} G_{\rm c}(\vec{p}, {\rm i}\epsilon_n) G_{\rm f}(\vec{p} + \vec{q}, {\rm i}\epsilon_n + {\rm i}\omega_m) \tag{47}$$

where $G_{\rm f}$ and $G_{\rm c}$ are the Matsubara Green function for f and conduction electrons, respectively. A dynamical response of (47) is expressed in terms of the spectral weight of the f electron as follows:

$$\chi_{\rm cf}^{(0)}(q, \omega) = \sum_{\vec{p}} \int \frac{{\rm d}x}{\pi} \int \frac{{\rm d}y}{\pi} {\rm Im}\, G_{\rm f}^{\rm R}(\vec{p} + \vec{q}, x) {\rm Im}\, G_{\rm c}^{\rm R}(\vec{p}, y) \frac{f(x) - f(y)}{\omega + y - x}, \tag{48}$$

where $f(x) = 1/({\rm e}^{x/T} + 1)$ is the Fermi distribution function, and the spectral weights ${\rm Im}\, G^{\rm R}$'s are given by

$${\rm Im}\, G_{\rm f}^{\rm R}(\vec{p} + \vec{q}, x) = \frac{\Sigma''_{\vec{p}+\vec{q}}(x)}{\left(x - \epsilon_{\rm f} - \Sigma'_{\vec{p}+\vec{q}}(x) - \frac{|V_{\vec{p}+\vec{q}}|^2}{x - \xi_{\vec{p}+\vec{q}}}\right)^2 + \left(\Sigma''_{\vec{p}+\vec{q}}(x)\right)^2}, \tag{49}$$

and

$${\rm Im}\, G_{\rm c}^{\rm R}(\vec{p}, y) = \frac{\Sigma''_{\vec{p}}(y)|V_{\vec{p}}|^2 \left[\left(M_{\vec{p}}(y)\right)^2 + \left(\Sigma''_{\vec{p}}(y)\right)^2\right]}{\left\{\left[\left(M_{\vec{p}}(y)\right)^2 + \left(\Sigma''_{\vec{p}}(y)\right)^2\right](y - \xi_{\vec{p}}) - |V_{\vec{p}}|^2 M_{\vec{p}}(y)\right\}^2 + |V_{\vec{p}}|^4 \left(\Sigma''_{\vec{p}}(y)\right)^2}, \tag{50}$$

where $\Sigma_p^{\rm R}(\epsilon) \equiv \Sigma'_p(\epsilon) + {\rm i}\Sigma''_p(\epsilon)$ is the f-electron self-energy function, and $M_{\vec{p}}(y) \equiv y - \epsilon_{\rm f} - \Sigma'_{\vec{p}}(y)$. It is noted that the q dependence of $\chi_{\rm cf}^{(0)}(q, \omega)$, (48), arises only through that of ${\rm Im}\, G_{\rm f}(\vec{p} + \vec{q}, x)$, (49). In heavy fermions, the self-energy Σ is almost local so that its wavenumber dependence can be safely neglected. Therefore, the q-dependence would arises through that of ξ (dispersion of conduction electron) and V (c–f hybridization). Since the f-electron spectral weight, (49), is dominated by the incoherent part around $x \sim \epsilon_{\rm f} - \mu < 0$ in the heavy fermion situation, the main contributions of p-summation and x-integration of (48) arise from the region $\xi_p > 0$ and $x \sim -|\mu - \epsilon_{\rm f}|$. Indeed, the weight of the coherent part associated quasiparticles (which would result in appreciable q dependence) amounts only to a

tiny contribution of the order of $z \sim m_{\rm band}/m^* \ll 1$. Thus, the q-dependence of $\chi_{\rm cf}^{(0)}(q,\omega)$ is estimated as

$$\chi_{\rm cf}(q,0) = \chi_{\rm cf}(0,0)\left[1 + \mathcal{O}\left(\frac{V}{|\mu-\epsilon_{\rm f}|}\right)^2\left(\frac{q}{q_{\rm c}}\right)^2\right] \tag{51}$$

where $q_{\rm c} \sim \pi/a$ with a being the lattice constant. In a typical heavy-fermion compound, $(V/|\mu-\epsilon_{\rm f}|)^2 < 10^{-1}$, the q-dependence of the valence susceptibility $\chi_{\rm v}$ is expected to be very small, consistent with microscopic calculations discussed in section 3.1.

5. Effect of magnetic field on valence transition

Roughly speaking, the valence-transition temperature $T_{\rm v}$ is expected to be influenced considerably by the magnetic field of the order of the effective Fermi energy $E_{\rm F}^*$. Therefore, in heavy-fermion metals, $T_{\rm v}$ is easily changed by a moderate magnetic field of the order of 10 T. Indeed, it has been reported recently that $T_{\rm v}$ of the α–γ transition in $Ce_{0.8}La_{0.1}Th_{0.1}$ vanishes in a magnetic field about 50 T [103]. Similarly, it is expected that the critical end point ($P_{\rm cr}$, $T_{\rm cr}$) also vanishes when enough magnetic field H is applied. Namely, it is expected that the QCP of the valence transition is induced by the magnetic field.

The H-dependence of $T_{\rm v}$ near the QCP is given as

$$T_{\rm v} \propto (H_{\rm v} - H)^{1/2}, \tag{52}$$

where $H_{\rm v}$ is the critical magnetic field. This is derived from the Clapeyron–Clausius relation on the (T, H) plane with the pressure P fixed:

$$\left(\frac{\partial T_{\rm v}}{\partial H}\right)_P = -\frac{(M_2 - M_1)}{(S_2 - S_1)} \tag{53}$$

where $M_{1(2)}$ and $S_{1(2)}$ are the magnetization and the entropy in the valence–fluctuation (Kondo) regime, respectively. In the low temperature limit ($T_{\rm v} \to 0$), $(S_2 - S_1) \propto T_{\rm v} > 0$, and $(M_2 - M_1) \sim$ constant > 0 because the specific heat and the susceptibility are larger in the Kondo regime (2) than the valence–fluctuation regime (1). Thus, equation (53) is approximated as

$$\frac{{\rm d}T_{\rm v}}{{\rm d}H} \sim -\frac{1}{T_{\rm v}}. \tag{54}$$

Then, near the critical magnetic field $H = H_{\rm v}$, the relation (52) is obtained.

The critical temperature $T_{\rm cr}$ of the end point will also vanish on applying magnetic field. In this case, the critical pressure $P_{\rm cr}$ changes simultaneously in general, so that the relation (52) cannot be applied directly. However, it is reasonable to expect a similar relation will hold:

$$T_{\rm cr}^2 \propto (H_{\rm cr} - H). \tag{55}$$

This gives an H-dependence of $T_{\rm cr}$ around the QCP of the valence transition. According to the spirit of the theory for the second order phase transition of Landau [104], the relation (55) is valid in the disordered state, for the regime of $T_{\rm cr} < 0$ in this case as long as the system is near the critical condition. Then, the QCP of the valence transition can be induced by the magnetic field available for the moment in such a system.

A potential candidate is $CeCu_6$. The pressure dependence of the coefficient A, the residual resistivity ρ_0, and $T_{\rm max}$, where the resistivity $\rho(T)$ takes a maximum, was reported by Raymond and Jaccard [105]. In figure 14, the relation between A and $T^{\rm max}$ of $CeCu_6$ for a series of pressures is displayed, together with those of $CeCu_2Si_2$ and $CeCu_2Ge_2$. The dashed curve is for $CeCu_6$. We can see that the valence changes rather sharply at around $T^{\rm max} = 100$ K, which

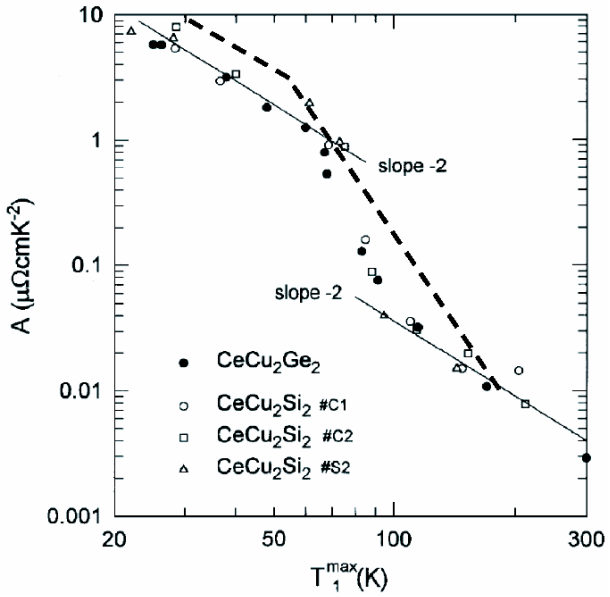

Figure 14. A versus $T^{\max}$ ($T_1^{\max}$) of $CeCu_6$ ($CeCu_2Si_2$ and $CeCu_2Ge_2$). Dashed lines are for $CeCu_6$ [105], filled circles are for $CeCu_2Ge_2$ and open symbols are for $CeCu_2Si_2$ [30].

corresponds to $P = 5$ GPa [105]. This clearly shows that $CeCu_6$ is a system near the QCP of the valence transition although its position is a bit distant from its QCP compared with the case of $CeCu_2Si_2$ and $CeCu_2Ge_2$. It is noted that the AF-QCP of $CeCu_6$ is induced by replacing Cu by Au [106], and seems to be located at $P = P_c \neq -0.3$ GPa [107]. Then, the pressure for the QCP of the valence transition is again about 5 GPa higher than that for the AF-QCP as in $CeCu_2(Si, Ge)_2$. The characteristic temperature T_F^* (or the effective Fermi energy ϵ_F^*) of $CeCu_6$ is very low, of the order of 10 K, reflecting the heaviness of its effective mass. Therefore, it is expected that the QCP is recovered by the magnetic field of the order of T_F^*, i.e., $H \sim 10$ T. The most interesting possibility is that the odd-parity superconductivity with equal-'spin' pairing may be promoted under the magnetic field $H \sim H_c$ because the pairing interaction induced by the CVF works between the quasiparticles at adjacent sites and is 'spin' independent.

The heavy-fermion compound $CeRu_2Si_2$, exhibiting metamagnetic behaviour, is also expected to exhibit a valence transition at $P \sim 4$ GPa, offering us another candidate for investigating the effect of magnetic field on valence transition [108].

Quite recently, the magnetic-field dependence of T_v has been discussed theoretically on the basis of the idea of the Kondo volume collapse [109]. However, as for the property associated with the QCP of the valence transition, there has been no theory of magnetic field so far to our knowledge. This problem certainly deserves to be explored in future study. According to preliminary calculations based on the $1/N$-expansion treatment of the model (3) with the magnetic field in the strongly correlated limit, the QCP of the valence transition is really promoted by magnetic fields [110, 111].

6. Generality of critical-valence–fluctuation mechanism of superconductivity

In previous sections it has been shown that the CVF of the Ce ion is a single origin for varieties of anomalous properties of $CeCu_2(Si, Ge)_2$ under pressure. The superconductivity realized at

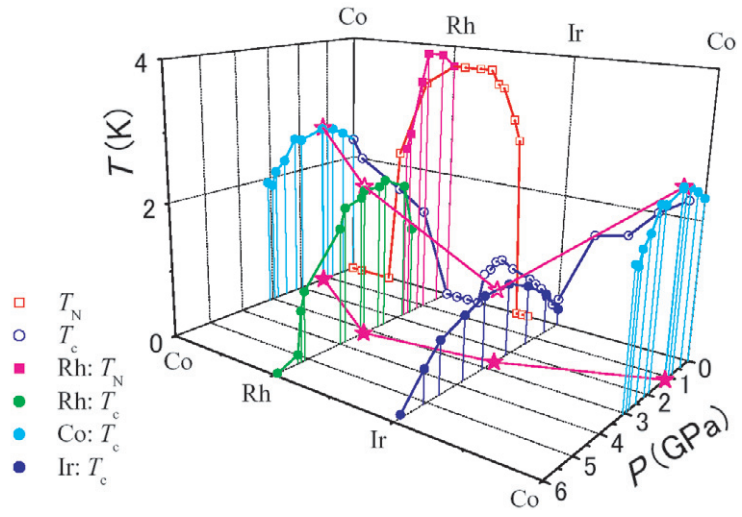

Figure 15. Phase diagram of Ce(Co, Rh, Ir)In_5 in P–T–x space.

$P \sim P_v$ is in a *high*-T_c state in the sense that T_c is of $\mathcal{O}(10^{-1})$ of the renormalized Fermi energy. In this sense, the critical-valence–fluctuation mechanism may offer one of the routes to the *room temperature superconductivity*. A natural question is whether there are other Ce-based systems in which the CVF plays an important role. In this section, some candidates are briefly discussed.

The properties of $CeTIn_5$ (T = Co, Rh, Ir) have the aspect similar to $CeCu_2(Si, Ge)_2$. Indeed, the P–T phase diagram of $CeRhIn_5$ is quite similar to that shown in figure 2 although the peak structure of T_c is less prominent. $\rho(T = T_c)$ exhibits a sharp peak structure at $P = P_{max}$ where T_c takes the maximum, and the temperature dependence of $\rho(T)$ follows an approximate T-linear behaviour [112, 113]. This similarity can be seen more clearly in figure 15, in which T_N and T_c are shown in P–T–x space, x being the concentration of $CeCo_{1-x}Rh_xIn_5$ ($0 \leqslant x \leqslant 1$), $CeRh_{2-x}Ir_{x-1}In_5$ ($1 \leqslant x \leqslant 2$), or $CeIr_{3-x}Co_{x-2}In_5$ ($2 \leqslant x \leqslant 3$) [14]. It is noted that the line of the magnetic QCP (P_c) is surrounded by the line of the T_c maximum around which $\rho \propto T$ behaviour is observed. This suggests that the T_c maximum is accompanied by the drastic valence change of the Ce ion.

From this point of view, the T-linear resistivity (at $T > T_c$) observed in $CeCoIn_5$ at ambient pressure should be attributed to nearly CVF rather than the two-dimensional antiferromagnetic critical fluctuations. Indeed, the latter point of view has difficulties in the following four points.

(i) Three dimensionality of the magnetic fluctuations cannot be neglected although the Fermi surface is in a quasi-cylindrical shape. Indeed, the anisotropy of the resistivity is only a few times which is far less than 6×10^2 in Sr_2RuO_4 [114], and 5×10^2 in high-T_c cuprates [115].

(ii) Even in two dimensions, it is rather difficult to derive T-linear resistivity because the electric current is carried mainly by the quasiparticles near the cold spot, which is not subject to the scattering of critical fluctuations [116, 117].

(iii) $CeCoIn_5$ is located off the magnetic critical point, which corresponds to $CeCo_{0.4}Rh_{0.6}In_5$ [14]. Very recent results of solid solution $CeCo(In, Cd)_5$ under pressure also suggest that the AF-QCP for $CeCoIn_5$ is located on the negative pressure side around $P = -0.6$ GPa [118]. Indeed, this can be easily understood if we realize the fact that 6.5% Cd doping is equivalent to applying pressure by 0.9 GPa, and that the AF-QCP is located

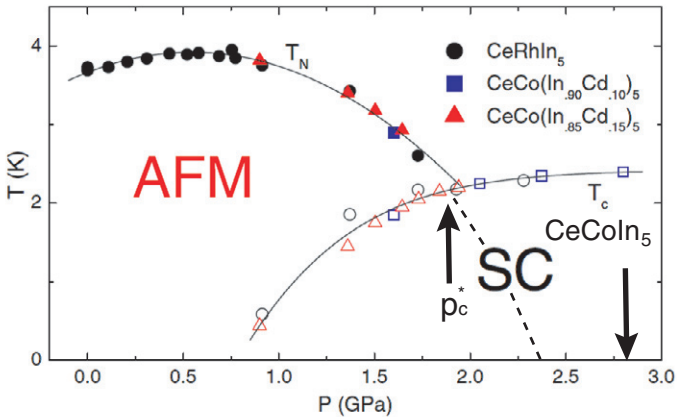

Figure 16. Phase diagram of Ce(Co, Rh)(In, Cd)$_5$ under pressure [118]. The dashed line represents a hypothetical Néel temperature realized if the superconducting state were absent [120, 121]. Consulting the phase diagram of CeCo(In, Cd)$_5$ in [118], CeCoIn$_5$ at ambient pressure is estimated to locate at $P = 2.8$ GPa in the CeRhIn$_5$ phase diagram as indicated by an arrow. $p_c^* \simeq 1.9$ GPa denotes the pressure where T_N and T_c coincide [120].

at pressure higher by 0.43 GPa than that where T_N and T_c coincide [118]. This situation can be seen in figure 16.

(iv) The residual resistivity exhibits a very drastic decrease on pressure application from $\rho_0 \simeq 3\ \mu\Omega$ cm at ambient pressure to $\rho_0 \simeq 0.2\ \mu\Omega$ cm at $P = 1.5$ GPa [119], suggesting the existence of the quantum CVT at $P \sim 0$. It is difficult to explain this phenomenon only from an effect of critical antiferromagnetic fluctuations [52]. It is noted here that $\rho_0 \simeq 3\ \mu\Omega$ cm corresponds to the mean free path of $\ell \sim 100$ Å of impurity scattering, which can cause a pseudogap behaviour as observed in experiment [119].

The importance of the CVF can be seen more clearly in the case of CeIrIn$_5$, in which the maximum of T_c is attained in the pressure region where the AF fluctuations are suppressed, as has been revealed by In^{115}-NQR measurement [122]. Two separated T_c domes have been observed under pressure in $CeIr_{3-x}Co_{x-2}In_5$ ($x = 0.8$) [123] as in $CeCu_2(Si_{0.9}Ge_{0.1})_2$ [36]. These facts strongly suggest that the CVF is developed in Ir-based compounds under pressure and at the origin of their *unconventional* behaviours.

It is also of interest to note that the recently discovered Pu-based superconductors PuCoGa$_5$ [124] and PuRhGa$_5$ [125] exhibit a trace of enhanced valence fluctuations. From a general point of view, 5f electrons in the Pu element itself are located near the boundary between the localized state with a nearly integral valence and the itinerant state with a fractional valence. Indeed, the systematic variation of the Wigner–Seitz radius for a series of actinide elemental metals clearly shows that the ionic radius changes drastically between Pu and Am metals, suggesting the existence of the valence fluctuations in metallic compounds including such elements associated with the 'valence transformation' [126].

Circumstantial evidence supporting this point of view is that the ratio A/γ^2, A being a coefficient of the T^2-term in the resistivity and γ the Sommerfeld coefficient, of these Pu115 compounds ($(A/\gamma^2) \simeq 3.4 \times 10^{-6}$ ($\mu\Omega$ cm (K^2 mol/mJ)^2) for PuCoGa$_5$ and $(A/\gamma^2) \simeq 2 \times 10^{-6}$ ($\mu\Omega$ cm (K^2 mol/mJ)^2) for PuCoGa$_5$ [127]) is between that for strongly correlated metals (the Kadowaki–Woods ratio, $(A/\gamma^2)_{KW} \simeq 1.0 \times 10^{-5}$, $\mu\Omega$ cm (K^2 mol/mJ)^2) and that for weakly correlated metals ($(A/\gamma^2) \simeq 0.4 \times 10^{-6}$, $\mu\Omega$ cm (K^2 mol/mJ)^2 [50]). This also suggests that Pu115 compounds are not strongly correlated metals near magnetic instability

but are subject to the valence fluctuations of the Pu ion, although the Sommerfeld coefficient ($\gamma \sim 77$ (mJ/K^2 mol) for $PuCoGa_5$ [124] and $\gamma \sim 95$ (mJ/K^2 mol) for $PuRhGa_5$ [125]) is moderately enhanced. The value of the A-coefficient is that of the zero temperature limit obtained where the superconductivity is destroyed by the magnetic field. Further circumstantial evidence is that the T dependence of the resistivity ρ is nearly linear as far as one can see in figure 3 of [124], although it is claimed in that paper that ρ increases approximately as $T^{1.35}$ at $T_c < T < 50$ K.

These anomalous aspects observed in Pu115 superconductors suggest a possibility that the high transition temperature ($T_c = 18.5$ K for $PuCoGa_5$ and $T_c = 9$ K for $PuRhGa_5$) is promoted at least in part by the enhanced valence–fluctuation of the Pu ion. It should be also noted that the AF fluctuations do not develop at all in these compounds, judging from the fact that NMR and NQR relaxation rates $1/T_1$ follow the Korringa law in rather wide temperature range [128, 129].

7. Prospects

We have retraced the development of the CVF mechanism of unconventional superconductivity, in which the role of Coulomb repulsion between f and conduction electrons was emphasized. We believe this mechanism is more general than first thought, as discussed in section 6.

Quite recently, Watanabe, Imada and the present author reported results [67] on the density-matrix-renormalization-group analysis for the one-dimensional (1D) version of the model Hamiltonian (3) in which the conduction band is given as

$$\epsilon_k = -t \sum_{i\sigma} (c^\dagger_{i\sigma} c_{i+1\sigma} + c^\dagger_{i+1\sigma} c_{i\sigma}), \tag{56}$$

where t is the nearest-neighbour hopping integral. For the electron number 7/4 per site, $V/t = 0.1$ and $U/t = 100$, a first order valence-transition line in the U_{fc}–ϵ_f plane has been determined, showing that the region of uniform phase is stabilized and phase separation is suppressed due to quantum fluctuations. On analysis of the exponent of the long-range behaviour of correlation functions of inter-site pairing, it has been shown that the superconducting correlation becomes dominant against CDW and SDW ones near the QCP of the valence transition in the region of uniform phase. This result supports the overall picture of CVF mediated unconventional superconductivity discussed in [33, 34, 37].

The effect of CVF on the longitudinal relaxation rate $1/T_1$ of NMR/NQR has not been discussed in the present paper. At first sight, valence fluctuation gives rise to no essential effect on $1/T_1$ since valence fluctuation is a sort of charge fluctuation, and is irrelevant to magnetic fluctuations. However, the dynamical susceptibility of the f electron $\chi^{\pm}_v(q, i\omega_m)$ corresponding to the spin-flip process is given in a form essentially similar to equation (46). Therefore, $\chi^{\pm}_v(q, i\omega_m)$ should be subject to a critical fluctuation associated with the valence transition, leading to an enhancement of $1/T_1$. This may be crucial to interpret the enhanced $1/T_1$ observed in Ce115 compounds away from the magnetic phase boundary.

Acknowledgments

The author is grateful to A Holmes, D Jaccard, H Maebashi, O Narikiyo and Y Onisih for their collaborations, on which this work is based. He has benefited very much from stimulating conversations with J Flouquet, S Fujimoto, K Hattori, H Ikeda, T Kasuya, S Kawasaki, Y Kitaoka, T C Kobayashi, G G Lonzarich, T Muramatsu, Y Nishida, A Onodera, F Steglich, A Tsuruta, C M Varma, S Watanabe, H-Q Yuan and G-q Zheng. This work was supported by

a Grant-in-Aid for COE research (No 10CE2004) by Monbusho, the Ministry of Education, Science, Sports and Culture of Japan.

References

[1] Anderson P W and Brinkman W F 1973 *Phys. Rev. Lett.* **30** 1108
[2] Nakjima S 1973 *Prog. Theor. Phys.* **50** 1101
[3] Steglich F, Aarts J, Bredl C D, Lieke W, Meschede D, Franz W and Schäfer H 1979 *Phys. Rev. Lett.* **43** 1892
[4] Miyake K, Schmitt-Rink S and Varma C M 1986 *Phys. Rev.* B **34** 6554
[5] Scalapino D J, Loh E Jr and Hirsch J E 1986 *Phys. Rev.* B **34** 8190
[6] Moriya T, Ueda K and Takahashi Y 1990 *J. Phys. Soc. Japan* **59** 2905
[7] Monthoux P and Pines D 1992 *Phys. Rev. Lett.* **69** 961
[8] Moriya T and Ueda K 2000 *Adv. Phys.* **49** 555
[9] Mathur N D, Grosche F M, Julian S R, Walker I R, Freye D M, Haselwimmer F K W and Lonzarich G G 1998 *Nature* **394** 39
[10] Grosche F M, Julian S R, Mathur N D and Lonzarich G G 1996 *Physica* B **223/224** 50
[11] Movshovich R, Graf T, Mandrus D, Thompson J D, Smith J L and Fisk Z 1996 *Phys. Rev.* B **53** 8241
[12] Monthoux P and Lonzarich G G 1999 *Phys. Rev.* **59** 14598
[13] Kohn W and Luttinger J M 1965 *Phys. Rev. Lett.* **15** 524
[14] Hotta T 1994 *J. Phys. Soc. Japan* **63** 4126
[15] Nomura T and Yamada K 2000 *J. Phys. Soc. Japan* **69** 3678
[16] Bauer E D, Frederick N A, Ho P-C, Zapf V S and Maple M B 2002 *Phys. Rev.* B **65** 100506(R)
[17] Tou H, Kitaoka Y, Ishida K, Asayama K, Kimura N, Ōnuki Y, Yamamoto E, Haga H and Maezawa K 1998 *Phys. Rev. Lett.* **80** 3129
[18] Tou H, Ishida K and Kitaoka Y 2005 *J. Phys. Soc. Japan* **74** 1245–54
[19] Yotsuhashi S, Miyake K and Kusunose H 2002 *Physica* B **312/313** 100
Yotsuhashi S and Miyake K 2002 unpublished
[20] Hasselbach K, Taillefer L and Flouquet J 1989 *Phys. Rev. Lett.* **63** 93
[21] Sato N K, Aso N, Miyake K, Shiina R, Thalmeier P, Varelogiannis G, Geibel C, Steglich F, Fulde P and Komatsubara T 2001 *Nature* **410** 340
[22] Miyake K and Sato N K 2001 *Phys. Rev.* B **63** 052508
[23] Saxena S S, Agarwal P, Ahilan K, Grosche F M, Hasselwimmer R K W, Steiner M J, Pugh E, Walker I R, Julian S R, Monthoux P, Lonzarich G G, Huxley A, Sheikin I, Braithwaite D and Flouquet J 2000 *Nature* **406** 587
[24] Huxley A, Sheikin I, Ressouche E, Kernavanois N, Braithwaite D, Calemczuk R and Flouquet J 2001 *Phys. Rev.* B **63** 144519
[25] Tateiwa N, Kobayashi T C, Hanazono K, Amaya K, Haga Y, Settai R and Ōnuki Y 2001 *J. Phys.: Condens. Matter* **13** L17
[26] Watanabe S and Miyake K 2002 *J. Phys. Soc. Japan* **71** 2489
[27] Bellarbi B, Benoit A, Jaccard D, Mignot J M and Braun H F 1984 *Phys. Rev.* B **30** 1182
[28] Thomas F, Ayache C, Fomin I A, Thomasson J and Geibel C 1996 *J. Phys.: Condens. Matter* **8** L51
[29] Jaccard D, Vargoz E, Alami-Yadri K and Wilhelm H 1998 *Rev. High Pressure Sci. Technol.* **7** 412
[30] Jaccard D, Wilhelm H, Alami-Yadri K and Vargoz E 1999 *Physica* B **259–261** 1
[31] Kobayashi T C, Miyazu T, Takeshita N, Shimazu K, Amaya K, Kitaoka Y and Ōnuki Y 1998 *J. Phys. Soc. Japan* **67** 996
[32] Kitaoka Y, Tou H, Zheng G-q, Ishida K, Asayama K, Kobayashi T C, Kohda A, Takeshita N, Amaya K, Ōnuki Y, Geibel C, Schank C and Steglich F 1995 *Physica* B **206/207** 55
[33] Miyake K, Narikiyo O and Onishi Y 1999 *Physica* B **259–261** 676
[34] Onishi Y and Miyake K 2000 *J. Phys. Soc. Japan* **69** 3955
[35] Miyake K and Maebashi H 2002 *J. Phys. Soc. Japan* **71** 1007
[36] Yuan H Q, Grosche F M, Deppe M, Geibel C, Sparn G and Steglich F 2003 *Science* **302** 2104
[37] Holmes A T, Jaccard D and Miyake K 2004 *Phys. Rev.* B **69** 024508
[38] Hegger H, Petrovic C, Moshopoulou E G, Hundley M F, Sarrao J L, Fisk Z and Thompson J D 2000 *Phys. Rev. Lett.* **84** 4986
[39] Petrovic C, Pagliuso P G, Hundley M F, Movshovich R, Sarrao J L, Thompson J D, Fisk Z and Monthoux P 2001 *J. Phys.: Condens. Matter* **13** L337

[40] Petrovic C, Movshovich R, Jaime M, Pagliuso P G, Hundley M F, Sarrao J L, Fisk Z and Thompson J D 2001 *Europhys. Lett.* **53** 354
[41] Pagliuso P G, Movshovich R, Bianchi A D, Nicklas M, Moreno N O, Thompson J D, Hundley M F, Sarrao J L and Fisk Z 2002 *Physica* B **312/313** 129
[42] Kawasaki Y, Ishida K, Obinata K, Yabuchi K, Kashima K and Kitaoka Y 2002 *Phys. Rev.* B **66** 224502
[43] Kawasaki S, Mito T, Kawasaki Y, Zheng G-q, Kitaoka Y, Aoki D, Haga Y and Ōnuki Y 2003 *Phys. Rev. Lett.* **91** 137001
[44] Balatsky A and Abrahams E 1992 *Phys. Rev.* B **45** 13125
Abrahams E, Balatsky A, Schrieffer J R and Allen P B 1993 *Phys. Rev.* B **47** 513
[45] Fuseya Y, Kohno H and Miyake K 2003 *J. Phys. Soc. Japan* **72** 2914
[46] Kuramoto Y and Miyake K 1990 *J. Phys. Soc. Japan* **59** 2381
[47] Rice T M and Ueda K 1986 *Phys. Rev.* B **34** 6420
[48] Shiba H 1986 *J. Phys. Soc. Japan* **55** 2765
[49] Kadowaki K and Woods S B 1986 *Solid State Commun.* **58** 507
[50] Miyake K, Matsuura T and Varma C M 1989 *Solid State Commun.* **71** 1149
[51] Rice M J 1968 *Phys. Rev. Lett.* **20** 1439
[52] Miyake K and Narikiyo O 2002 *J. Phys. Soc. Japan* **71** 867
[53] Onodera A, Tsuduki S, Ohishi Y, Watanuki T, Ishida K, Kitaoka Y and Ōnuki Y 2002 *Solid State Commun.* **123** 113
[54] Fisk Z, Thompson J D, Lawrence J M, Smith J L and Batlogg B 1984 *J. Appl. Phys.* **55** 1921
[55] For review at early stage, see for example Varma C M 1976 *Rev. Mod. Phys.* **48** 219
[56] Haldane F D M 1978 *Phys. Rev. Lett.* **40** 416
[57] Falicov L M and Kimball J C 1969 *Phys. Rev. Lett.* **22** 997
[58] Khomskii D I and Kocharjan A N 1976 *Solid State Commun.* **18** 985
[59] Aliscio B, Allub R and Balseiro C A 1986 *Phys. Rev.* B **34** 4786
[60] Costi T A and Hewson A C 1991 *Physica* C **185–189** 2649
Costi T A and Hewson A C 1992 *J. Magn. Magn. Mater.* **108** 108
[61] Hewson A C 1993 *The Kondo Problem to Heavy Fermions* (Cambridge: Cambridge University Press)
[62] Takayama R and Sakai O 1997 *J. Phys. Soc. Japan* **66** 1512
Shimizu Y 1997 private communications
[63] Gonçalves da Silva C E T and Falicov L M 1975 *Solid State Commun.* **17** 1521
[64] Hewson A C and Riseborough P S 1977 *Solid State Commun.* **22** 379
[65] Singh I, Ahuja A K and Joshi S K 1980 *Solid State Commun.* **34** 65
[66] Onishi Y and Miyake K 2000 *Physica* B **281/282** 191
[67] Watanabe S, Imda M and Miyake K 2006 *J. Phys. Soc. Japan* **75** 043710
[68] Varma C M, Schmitt-Rink S and Abrahams E 1987 *Solid State Commun.* **62** 681
[69] Hirashima D S, Ōno Y, Matsuura T and Kuroda Y 1992 *J. Phys. Soc. Japan* **61** 649
[70] Brandow B H 1994 *Int. J. Mod. Phys.* B **8** 2667
Brandow B H 1994 *Int. J. Mod. Phys.* B **8** 3859
[71] Read R and Newns D M 1983 *J. Phys. C: Solid State Phys.* **16** 3273
[72] Read R and Newns D M 1983 *J. Phys. C: Solid State Phys.* **16** L1055
[73] Millis A J and Lee P A 1986 *Phys. Rev.* B **35** 3394
[74] Auerbach A and Levin K 1986 *Phys. Rev. Lett.* **57** 877
[75] Lavagne M, Millis A J and Lee P A 1987 *Phys. Rev. Lett.* **58** 266
[76] Houghton A, Read N and Won H 1987 *Phys. Rev.* B **37** 3782
[77] Riseborough P S 1998 *Phys. Rev.* B **58** 15534
[78] Onishi Y and Miyake K 1999 *J. Phys. Soc. Japan* **68** 3927
[79] Miyake K, Matsuura T, Jichu H and Nagaoka Y 1984 *Prog. Theor. Phys.* **72** 1063
[80] Ikeda H 2002 *J. Phys. Soc. Japan* **71** 1126
[81] Takimoto T, Hotta T, Maehira T and Ueda K 2002 *J. Phys.: Condens. Matter* **14** L369
[82] Okada I and Yosida K 1973 *Prog. Theor. Phys.* **49** 1483
[83] Yamada K, Yosida K and Hanzawa K 1984 *Prog. Theor. Phys.* **71** 450
[84] Nishida Y, Tsuruta A and Miyake K 2006 *J. Phys. Soc. Japan* **75** 064706
[85] Varma C M, Littlewood P B, Schmitt-Rink S, Abrahams E and Ruckenstein A E 1989 *Phys. Rev. Lett.* **63** 1996
[86] Perakis I E, Varma C M and Ruckenstein A E 1993 *Phys. Rev. Lett.* **70** 3467
[87] Varma C M, Nussinov Z and van Saarloos W 2002 *Phys. Rep.* **361** 267
[88] Sereni J G 1995 *Physica* B **215** 273
[89] Betbeder-Matibet O and Nozières P 1966 *Ann. Phys.* **37** 17

[90] Kotliar G, Abrahams E, Ruckenstein A E, Varma C M, Littlewood P B and Schmitt-Rink S 1991 *Europhys. Lett.* **15** 655
[91] Varma C M 1997 *Phys. Rev. Lett.* **97** 1535
[92] Miyake K and Maebashi H 2001 *J. Phys. Chem. Solids* **62** 53
[93] Maebashi H, Miyake K and Varma C M 2002 *Phys. Rev. Lett.* **88** 226403
[94] Maebashi H, Miyake K and Varma C M 2005 *Phys. Rev. Lett.* **95** 207207
[95] Abrikosov A A, Gorkov L P and Dzyaloshinskii I Ye 1965 *Quantum Field Theoretical Methods in Statistical Physics* 2nd edn (Oxford: Pergamon) section 19.3
[96] Langer J S 1961 *Phys. Rev.* **124** 1003
[97] Friedel J 1952 *Phil. Mag.* **43** 153
Friedel J 1958 *Nuovo Cimento Suppl.* **7** 287
[98] Langer J S and Ambegaokar V 1961 *Phys. Rev.* **121** 1090
[99] Dionicio G 2005 private communication
[100] Hertz J A 1976 *Phys. Rev.* B **14** 1165
[101] Hattori K and Miyake K 2006 unpublished
[102] Moriya T 1985 *Spin Fluctuations in Itinerant Electron Magnetism* (*Springer Series of Solid State Sciences* vol 56) (Berlin: Springer) chapter 4
[103] Drymiotis F, Singleton J, Harrison N, Balicas L, Bangura A, Mielke C H, Fisk Z, Migliori A, Smith J L and Lashley J C 2005 *J. Phys.: Condens. Matter* **17** L77
[104] Landau L D 1937 *JETP* **7** 19
Landau L D 1937 *Phys. Z. Sowjet* **11** 26
[105] Raymond S and Jaccard D 2000 *J. Low Temp. Phys.* **120** 107
[106] von Löhneysen H 1996 *J. Phys. C: Solid State Phys.* **8** 9689
[107] Flouquet J 2006 private communication
[108] Flouquet J, Haga Y, Haen P, Braithwaite D, Knebel G, Raymond S and Kambe S 2004 *J. Magn. Magn. Mater.* **272–276** 27
[109] Basu S and Riseborough P S 2006 *Physica* B **378–380** 686
[110] Tsuruta A 2006 private communication
[111] Watanabe S 2006 private communication
[112] Muramatsu T, Tateiwa N, Kobayashi T C, Shimizu K, Amaya K, Aoki D, Shishido H, Haga Y and Ōnuki Y 2001 *J. Phys. Soc. Japan* **70** 3362
[113] Muramatsu T 2001 private communication
[114] Hussey N E, Mackenzie A P, Cooper J R, Maeno Y, Nishizaki S and Fujita T 1998 *Phys. Rev.* B **57** 5505
[115] Uchida S, Ido T, Takagi H, Arima T, Tokura Y and Tajima S 1991 *Phys. Rev.* B **43** 7942
[116] Fujimoto S, Kohno H and Yamada K 1991 *J. Phys. Soc. Japan* **60** 2724
[117] Hlubina R and Rice T M 1995 *Phys. Rev.* B **51** 9253
[118] Pham L D, Park T, Maquilon S, Thompson J D and Fisk Z 2006 *Phys. Rev. Lett.* **97** 056404
[119] Sidorov V A, Nicklas M, Pagliuso P G, Sarrao J L, Bang Y, Balatsky A V and Thompson J D 2002 *Phys. Rev. Lett.* **89** 157004
[120] Knebel G, Aoki D, Braithwaite D, Salce S and Flouquet J 2006 *Phys. Rev.* B **74** 020501
[121] Park T, Ronning F, Yuan H Q, Salamon M B, Movshovich R, Sarrao J L and Thompson J D 2006 *Nature* **440** 65
[122] Kawasaki S, Zheng G-q, Kan H, Kitaoka Y, Shishido H and Ōnuki Y 2005 *Phys. Rev. Lett.* **94** 037007
[123] Nicklas M, Sidorov V A, Borges H A, Pagliuso P G, Sarrao J L and Thompson J D 2004 *Phys. Rev.* B **70** 020505
[124] Sarrao J L, Morales L A, Thompson J D, Scott B L, Stewart G R, Wastin F, Rebizant J, Boulet P, Colineau E and Lander G H 2002 *Nature* **420** 297
[125] Wastin F, Boulet P, Rebizant J, Colineau E and Lander G H 2003 *J. Phys.: Condens. Matter* **15** S2279
[126] Cooper N G (ed) 2000 *Challenges in Plutonium Science* Los Alamos Science No. 26
[127] Wastin F 2002 private communication
[128] Curro N J, Caldwell T, Bauer E D, Morales L A, Graf M J, Bang Y, Balatsky A V, Thompson J D and Sarrao J L 2005 *Nature* **434** 622
[129] Sakai H, Tokunaga Y, Fujimoto T, Kambe S, Walstedt R E, Yasuoka H, Aoki D, Homma Y, Yamamoto E, Nakamura A, Shiokawa Y, Nakajima K, Arai Y, Matsuda T D, Haga Y and Ōnuki Y 2005 *J. Phys. Soc. Japan* **74** 1710